DEPARTMENT OF MATHEMATICS

COMPRESSIBLE FLOW IN DUCTS

- ANALYTIC ASPECTS

J WIXCEY

Numerical Analysis Report 12/88

UNIVERSITY OF READING

COMPRESSIBLE FLOW IN DUCTS - ANALYTIC ASPECTS

J. R. WIXCEY

NUMERICAL ANALYSIS REPORT 12/88

Department of Mathematics
P.O. Box 220
University of Reading
Whiteknights
Reading
RG6 2AX
United Kingdom

This work forms part of the research programme of the Institute of Computational Fluid Dynamics at the Universities of Oxford and Reading and has been supported by the S.E.R.C.

CONTENTS

ABSTRACT

This report is the first of three that will consider the analysis of fluid flow through axi-symmetric ducts (inclusive of de-Laval nozzle flow) by its reduction to an approximate quasi one-dimensional flow. The qualitative behaviour of the flow variables is discussed and detailed calculations carried out to show graphically the flow variable variation throughout the duct for particular cases of both subsonic and supersonic flow.

ACKNOWLEDGEMENTS

I am grateful to Dr. M.J. Baines and Dr. D. Porter for their assistance in this work and their patience in waiting for this report.

I acknowledge an S.E.R.C. research studentship.

INTRODUCTION

This is the first of three reports in which we discuss the exact and approximate solution of a particular problem in fluid mechanics by using variational principles and finite element methods. The problem to be considered is steady compressible gas flow through various types of duct, and in this report we specify the form of the problem and obtain detailed solutions for later comparison. This will give a firm foundation for future work.

Thus in Section one the properties of the full compressible flow to be considered are stated and algebraic relations derived (see [2]) between the mechanical flow variables associated with the motion of a fluid particle on a streamline in the flow field.

In Section two the concept of duct flow is introduced together with the duct types to be considered. The reduction to an approximate quasi one-dimensional form, in which a single streamline represents the full flow [3], is presented.

The first two sections are then linked together in Section three in the discussion of graphical representations of the relationships between flow variables holding for a particle moving on the duct representative streamline, and hence throughout the actual quasi one-dimensional duct flow.

Finally in Section four the combination of the theory of Section two and the treatment of Section one for a general flow leads to a convenient parameterization of the approximate duct flow, through a point-wise non-linear relationship between fluid speed and distance along the duct axis. A basis for comparison with the numerical approximations of the two later reports is therefore obtained.

SECTION ONE : COMPRESSIBLE FLOW

1.1 FLOW HYPOTHESIS

The purpose of this section is to define the properties of the flow to be considered. Algebraic relations between the mechanical flow variables associated with a particle moving on a streamline in the flow field are then derived (cf.[2]) and subsequently these are represented graphically.

The fluid

The fluid in which the flow occurs is assumed to be a polytropic gas and has associated with it a set of thermodynamic equations. Such a gas satisfies the law of Boyle and Gay-Lussac expressed by the equation of state

$$p\,\nu = \left[R_o/m\right] T \ , \tag{1.1}$$

where p indicates pressure, T temperature, m the molecular weight of the gas and R_o the universal gas constant. The quantity ν, the specific volume, is defined by

$$\nu = (1/\rho) \ , \tag{1.2}$$

where ρ is density.

Taking the specific heat capacity at constant volume, c_v, defined by

$$c_v = \frac{R_o}{m\,(\gamma-1)} \,, \tag{1.3}$$

to be constant, where γ is the adiabatic exponent associated with the medium, then in the present case the internal energy, U, of the medium

$$U = c_v\, T \,, \tag{1.4}$$

is proportional to the temperature. Using (1.3) and in addition combining (1.4) with (1.1) yields the entropic equation of state,

$$p = \eta\, \rho^{\gamma} \,, \tag{1.5}$$

for the fluid medium (see [1]) where η is a function of entropy S. Again using (1.3) we can define the entropy function

$$\eta(S) = \left[R_o/m\right] \exp\left[\, \left[m/c_v\right] \left[S-S_o\right] \,\right] \,, \tag{1.6}$$

where S_o is a datum constant, and the internal energy

$$U = \left[\, \eta(S) \,/\, (\gamma-1) \,\right] \rho^{\gamma-1} \,. \tag{1.7}$$

The equation set (1.5) [with (1.6)] and (1.7) form the thermodynamic equations associated with the fluid considered.

Flow definition

The assumptions associated with the fluid flow are now given. On considering the fluid to be inviscid and neglecting heat conduction the entropy at a fluid particle remains constant throughout the motion, i.e. the changes in state at the particle are adiabatic so that

$$\frac{DS}{Dt} = 0 \ , \qquad (1.8)$$

where t is time and D/Dt denotes the material derivative.

If the motion is furthermore assumed to be steady so that the fluid speed, pressure, density and entropy are unchanged in time at each point, then the flow has the property that all fluid particles passing through a particular point in the flow field will have the same values of these quantities and subsequently follow the same path, the streamline, through that point.

The flow can therefore be described by streamlines invariant in time. A consequence of these assumptions is that not only is the entropy, S, constant at a fluid particle but it is a constant for each streamline throughout the flow field. Hence the entropy function, $\eta(S)$, itself is therefore also constant for each streamline.

1.2 EQUATIONS OF MOTION

The motion of the fluid is governed by the steady form of the conservation equations of fluid dynamics,

CONSERVATION OF MASS : $$\nabla.(\rho\, v) = 0 \,, \qquad (1.9)$$

CONSERVATION OF MOMENTUM : $$\nabla p + \rho\, (v.\nabla)\, v = 0 \,, \qquad (1.10)$$

CONSERVATION OF ENERGY : $$\rho\, v\, \nabla\, U + p\, \nabla\, v = 0 \,, \qquad (1.11)$$

where v is the fluid speed and ∇ the gradient operator, together with the equation of state (1.5).

The conservation of energy equation (1.11) may be simplified, through substitution of (1.9), to a form reflecting the fact that the changes of state are adiabatic

ADIABATIC CHANGES OF STATE : $$v.\nabla\, S = 0 \,. \qquad (1.12)$$

The momentum equation (1.10) can be rewritten in the form,

$$\nabla\, (\, U + [p/\rho] + [v^2/2]\,) - T\, \nabla\, S = v \times (\nabla \times v) \,, \qquad (1.13)$$

and subsequently, by enforcing (1.12), as an explicit relationship holding on a streamline in the flow field (see [2])

$$U + [p/\rho] + [v^2/2] = \text{CONSTANT ON A STREAMLINE} . \qquad (1.14)$$

The integration constant of (1.14) is the total energy per unit mass available to a particle moving on a streamline in the fluid, h. This then becomes the steady form of Bernouilli's equation that holds on the streamline in the flow field

$$U + [p/\rho] + [v^2/2] = h . \qquad (1.15)$$

1.3 RELATIONS BETWEEN FLOW VARIABLES

Attention is now confined to the motion of a fluid particle on a single streamline in the flow field. In addition to pressure, fluid speed, temperature and density, that have been defined previously, we introduce mass flow rate, Q, and flow stress, P, defined by

$$Q = \rho v \qquad (1.16)$$

and

$$P = p + \rho v^2 . \qquad (1.17)$$

For an ideal gas algebraic relations between pairs of these thermodynamic and mechanical flow variables collectively holding for a particle as it moves on a streamline in any flow field, in up to three dimensions, have been derived in [2]. These relations hold for any fluid particle moving on the streamline irrespective of its detailed motion.

Firstly, direct substitution of the thermodynamic equations (1.5) and (1.7) into Bernouilli's equation (1.15) yields a relationship between pressure and fluid speed for a particle moving on the streamline,

$$p(v) = \eta^{(1/(1-\gamma))} \left[[(\gamma-1)/\gamma] \, [h-(v^2/2)] \right]^{(\gamma/\gamma-1)} , \qquad (1.18)$$

specified through assigned constant values of entropy, defined by (1.6), and total energy per unit mass.

Before progressing to the derivation of the other relations it is convenient at this point to define certain significant fluid speeds.

There is a maximum limit speed, v_L, which a particle can attain in its motion on each streamline. This speed is approached as the density tends to zero and is

$$v_L = (2\,h)^{\frac{1}{2}} , \qquad (1.19)$$

defined solely in terms of the total energy (see [1]). It is apparent from (1.18) that the limit is necessary so that the pressure remains real.

The most significant fluid speed that may be attained by the particle moving on the streamline is the critical speed, C_*. This is the speed at which the fluid speed equals the local sound speed and divides

the streamline into segments of subsonic and supersonic flow (see [1]), i.e.

$$v < C_* \quad : \quad \text{SUBSONIC FLOW} \ , \qquad (1.20)$$

$$v > C_* \quad : \quad \text{SUPERSONIC FLOW} \ .$$

C_* is defined through the introduction of a constant, μ, related to the adiabatic exponent γ,

$$\mu = (\gamma-1)/(\gamma+1) \ , \qquad (1.21)$$

and the limit speed (1.19) attainable on the streamline (see [1]):

$$C_* = \mu \, v_L \ . \qquad (1.22)$$

Therefore note that for the flow of a steady polytropic gas the critical speed is independent of entropy.

Returning to the algebraic relations, subsequent to the definition of (1.18), the relations between the fluid speed and remaining flow variables may be obtained through (1.1), (1.5), (1.16) and (1.17):

$$T(v) = \left[m/R_o\right] \left[(\gamma-1)/\gamma\right] \left[h-[v^2/2]\right] \ , \qquad (1.23)$$

$$\rho(v) = \eta^{(1/(1-\gamma))} \left[\, [(\gamma-1)/\gamma] \, [h-(v^2/2)] \, \right]^{(1/(\gamma-1))} \ , \qquad (1.24)$$

$$Q(v) = \eta^{(1/(1-\gamma))}\, v \left[[(\gamma-1)/\gamma]\, [h-(v^2/2] \right]^{(1/(\gamma-1))} , \quad (1.25)$$

$$P(v) = \eta^{(1/(1-\gamma))} \left[[(\gamma-1)/\gamma]\, [h-(v^2/2)] + v^2 \right] \quad (1.26)$$
$$\left[[(\gamma-1)/\gamma]\, [h-(v^2/2)] \right]^{(1/(\gamma-1))} .$$

The critical values of all of the mechanical flow variables, corresponding to particle motion on a particular streamline, can now be obtained through substitution of the critical fluid speed into the full set of algebraic relations (1.18) and (1.23)-(1.26). Furthermore these relations can be used to provide, through the fluid speed, a particular parameterization of the relationships between the mechanical flow variables.

1.4 GRAPHS OF ALGEBRAIC RELATIONSHIPS

Specification of the fluid and the choice of streamline parameters allows graphical representation of the algebraic relations (1.18) and (1.23)-(1.26) between the flow variables, p, v, ρ, T, Q and P.

The adiabatic constant for most gases lies in the range $1 \rightarrow 5/3$. In the present case the fluid is considered to be air, which at moderate temperatures can be assumed to be polytropic. The associated thermodynamic constants are then given as in [2] by

$$\gamma = 1.4 \ , \tag{1.27}$$

$$m = 28.96 \times 10^{-2} \text{ kg} \ , \tag{1.28}$$

and

$$R_o = 8.31 \text{ Jmol}^{-1}\text{K}^{-1} \ . \tag{1.29}$$

For the isolation of a particular streamline it is necessary to assign constant values of entropy, S, and total energy, h. The entropy value is taken to be that at standard temperature and pressure,

$$\eta = 7.08 \times 10^{4} \text{ (SI UNITS)} \ , \tag{1.30}$$

and the total energy value that at standard temperature and zero fluid speed

$$h = 2.74 \times 10^{5} \text{ Jmol}^{-1}\text{kg}^{-1} \ . \tag{1.31}$$

It is now possible to compute the limit speed (1.19) and critical speed (1.22) attainable by a particle on this particular streamline, these becoming

$$v_L = 740.3 \text{ ms}^{-1} \tag{1.32}$$

and

$$C_* = 302.5 \text{ ms}^{-1} \ . \tag{1.33}$$

Furthermore, the magnitude of the critical values of the remaining flow variables on this streamline may be found from (1.18) and (1.23)-(1.26), namely,

$$p_* = 53100.13696 ,$$
$$T_* = 227.26593 ,$$
$$\rho_* = 0.81425 , \qquad (1.34)$$
$$Q_* = 246.31124 ,$$
and $$P_* = 127608.9692 .$$

Given a uniformly increasing discrete set of fluid speed values,

$$0 \leq v_i \leq v_L \qquad i = 1(1)101 , \qquad (1.35)$$

(see FIG.1*i*) the variation of the remaining dependent flow variables may be obtained from the algebraic relations (1.18) and (1.23)-(1.26). These are represented graphically in FIG.1. Further, using the fluid speed as an intermediate numerical parameter, graphical representation of the relationships between any other pair of mechanical flow variables may be found (FIG.2).

Note that a particular motion may be represented as a sub-set of points on each of the graphs (FIGS.1,2) and that only a portion of each graph is in general necessary to define completely the relative variation of each mechanical flow variable pair throughout that entire motion.

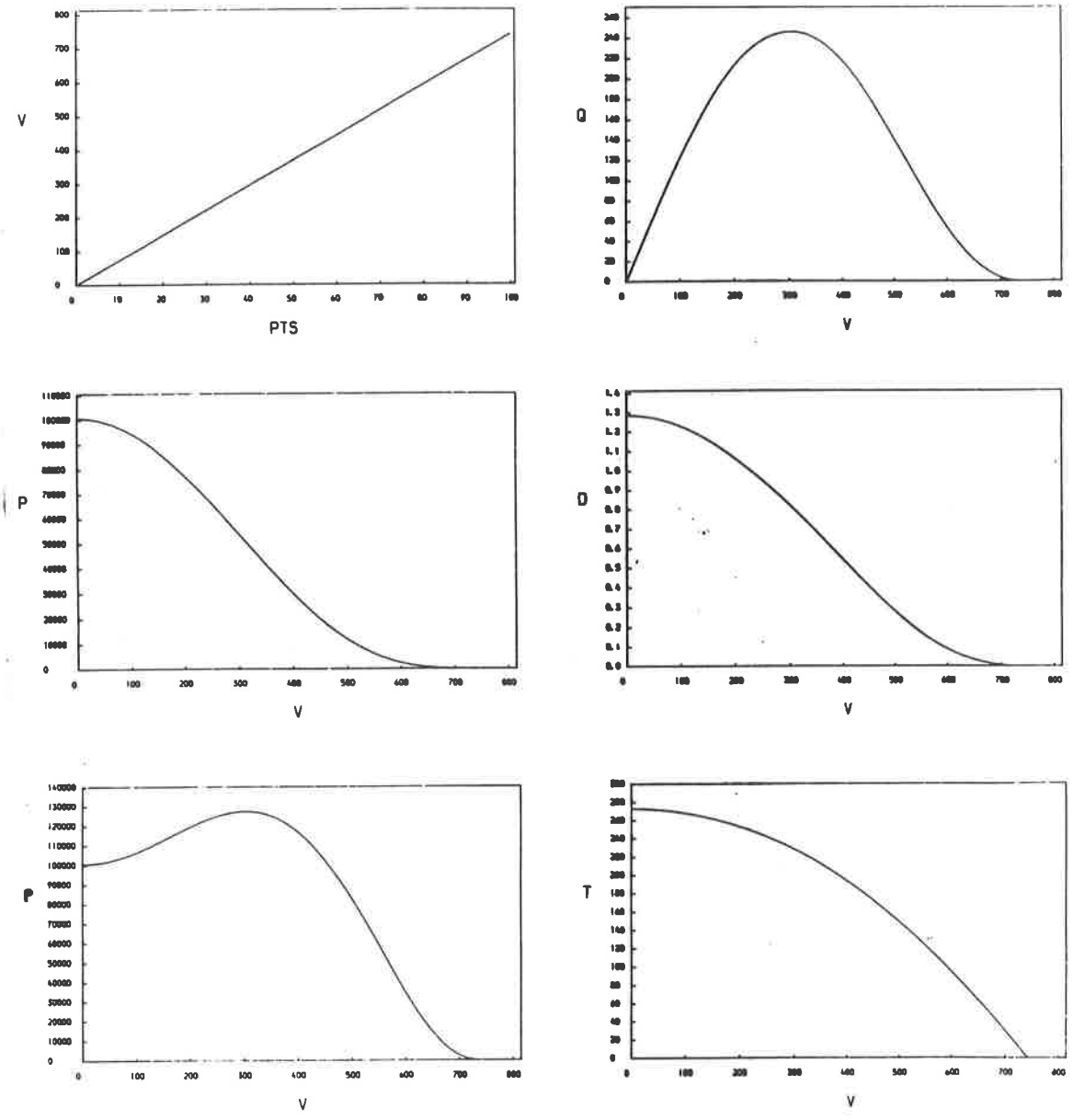

FIG.1

GRAPHICAL REPRESENTATION OF RELATIONSHIPS BETWEEN FLOW VARIABLE PAIRS

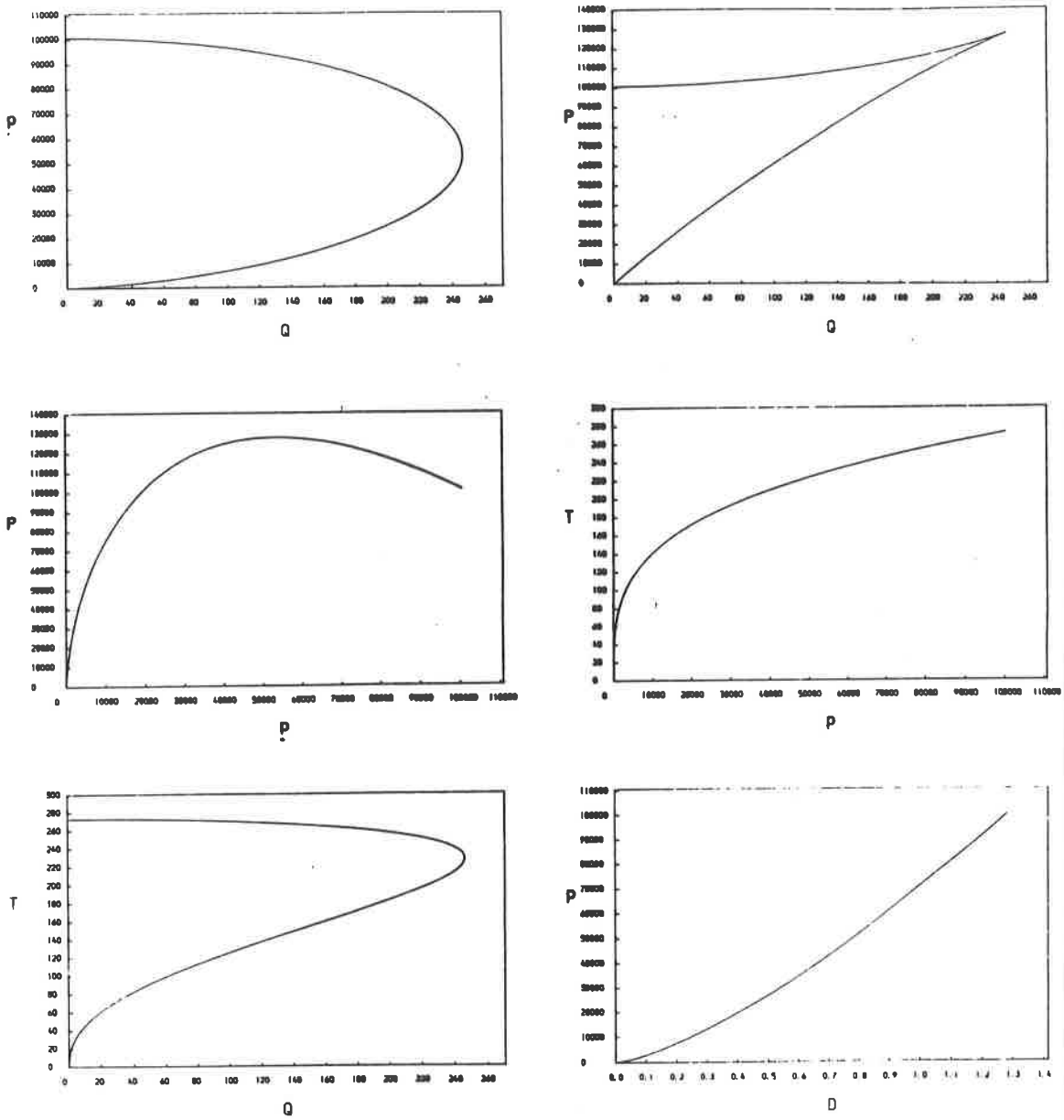

FIG TWO

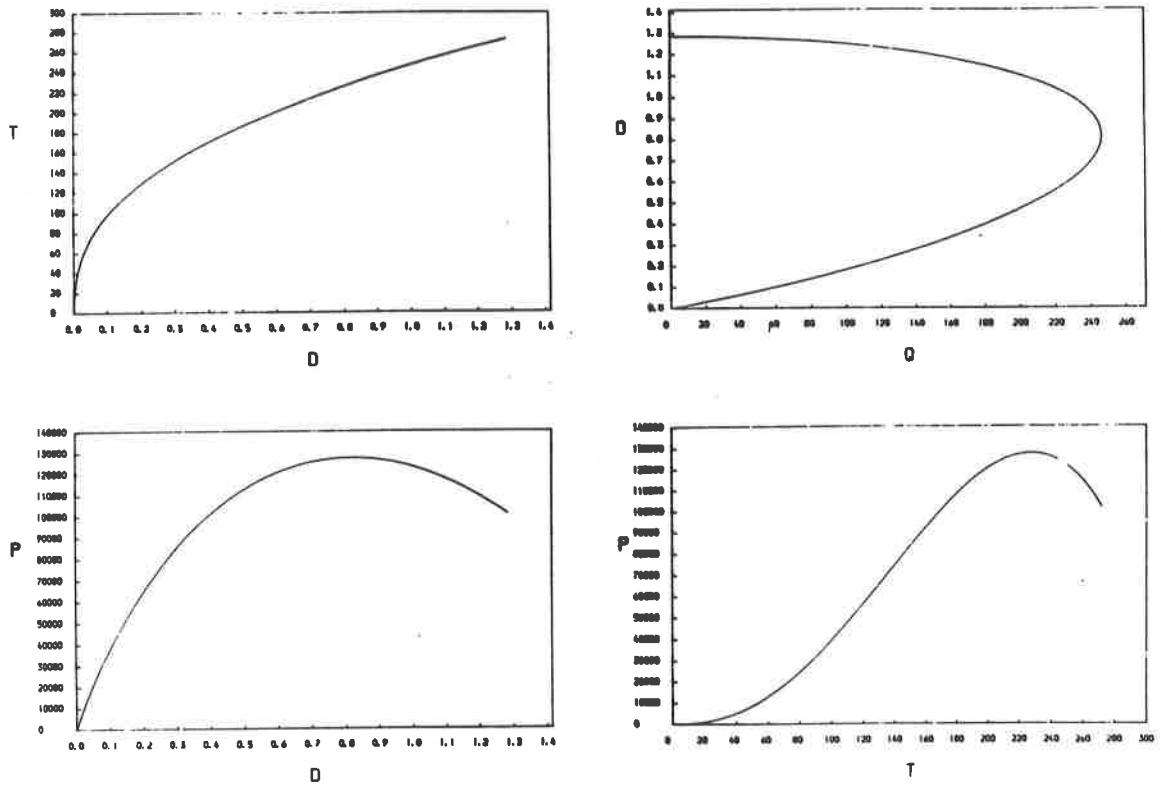

FIG TWO

cont

SECTION TWO : A PARTICULAR MOTION

The analysis is now confined to a specific example of compressible flow, governed by equations (1.9), (1.10) and (1.12). The motion to be studied is the flow of air, modelled by the polytropic gas, through various types of duct.

2.1 DUCT FLOW

We consider firstly flow through either a converging or diverging cone section which is cylindrically symmetrical about its axis (FIG.3*i*,*ii*). The discussion then proceeds to consideration of a duct type of great practical importance by taking a particular combination of the section forms shown in FIG.3*i*,*ii* which are connected in a manner so as to form an axi-symmetric de-Laval nozzle, with a single point of minimum area known as the nozzle throat (FIG.3*iii*).

An additional assumption made here about the duct flow is that it be homentropic, so that the entropy is constant throughout the flow field, except at discontinuities such as shocks. The energy equation in the form (1.12) is then satisfied identically. As for the general flow, the duct flow field can be thought of as consisting of streamlines invariant in time.

Boundary conditions must be supplied to fully define the motion. The inlet duct boundary condition is prescribed as stated in [3].
It is assumed that a 'control surface' can be positioned in the flow field at duct entry, across which the fluid velocity vector is orthogonal. The mass flow rate, Q_e, and total energy, h_e, at entry are then assigned across this surface as functions of position.

Since Bernouilli's equation (1.15) holds on the streamlines in the flow field (§1), a fluid particle moving on such a streamline will always have associated with it the total energy value at entry, assigned at the streamline entrance to the duct via the control surface.

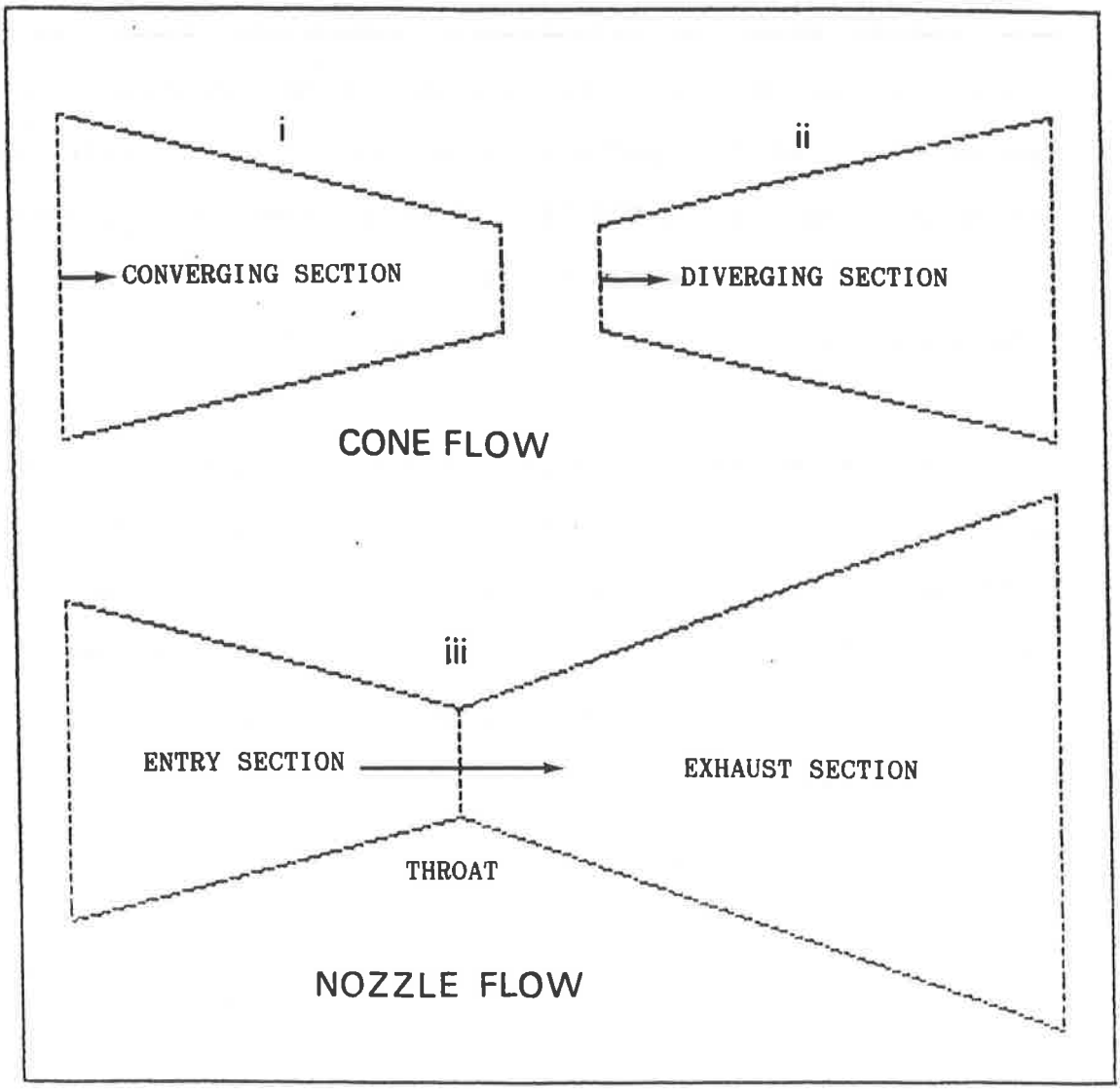

FIG THREE

2.2 QUASI ONE-DIMENSIONAL DUCT FLOW

The aim here is the reduction of the full flow (§2.1), by the use of a quasi one-dimensional approximation, to consideration of a single representative streamline on which the particle history typifies the particular duct flow. An outline of this process is given in [3], but is also presented here for convenience.

Quasi one-dimensional approximation

Recalling that the duct is axi-symmetric, introduce first the notation,

x : Distance along the axis of the duct from the entry station.

A(x) : Area of surface, possibly curved, at x orthogonal to every streamline in the flow field.

Now introduce a quantity, $\bar{Q}(x)$, the average mass flow rate across the transverse surface of area A(x). This, through,

$$\bar{Q}(x)\, A(x) = \int_A Q \, dA \,, \qquad (2.1)$$

defines the quasi one-dimensional approximation, where the integration is over that surface.

The motion equation (1.9) is now replaced by the form implied by (2.1) applicable to this approximation to duct flow, namely

$$\frac{d}{dx}(\bar{Q}\,A) = 0 \,. \tag{2.2}$$

Integrating (2.2) in the present case yields a local explicit relationship,

$$\bar{Q}(x) = \frac{C\,A_e}{A(x)} \,, \tag{2.3}$$

where $$C\,A_e = \int_{A_e} Q_e \, dA_e \,, \tag{2.4}$$

between the average mass flow rate and the associated transverse surface, where A_e is the area of the entry surface to the duct and Q_e is the duct entry mass flow rate.

The constant C in (2.3) can now be interpreted, by comparing (2.4) with (2.1), as the average mass flow rate across the duct entry surface.

The quasi one-dimensional approximation is shown in FIG.4 applied to the approximation of flow through a de-Laval nozzle.

QUASI ONE-DIMENSIONAL APPROXIMATION

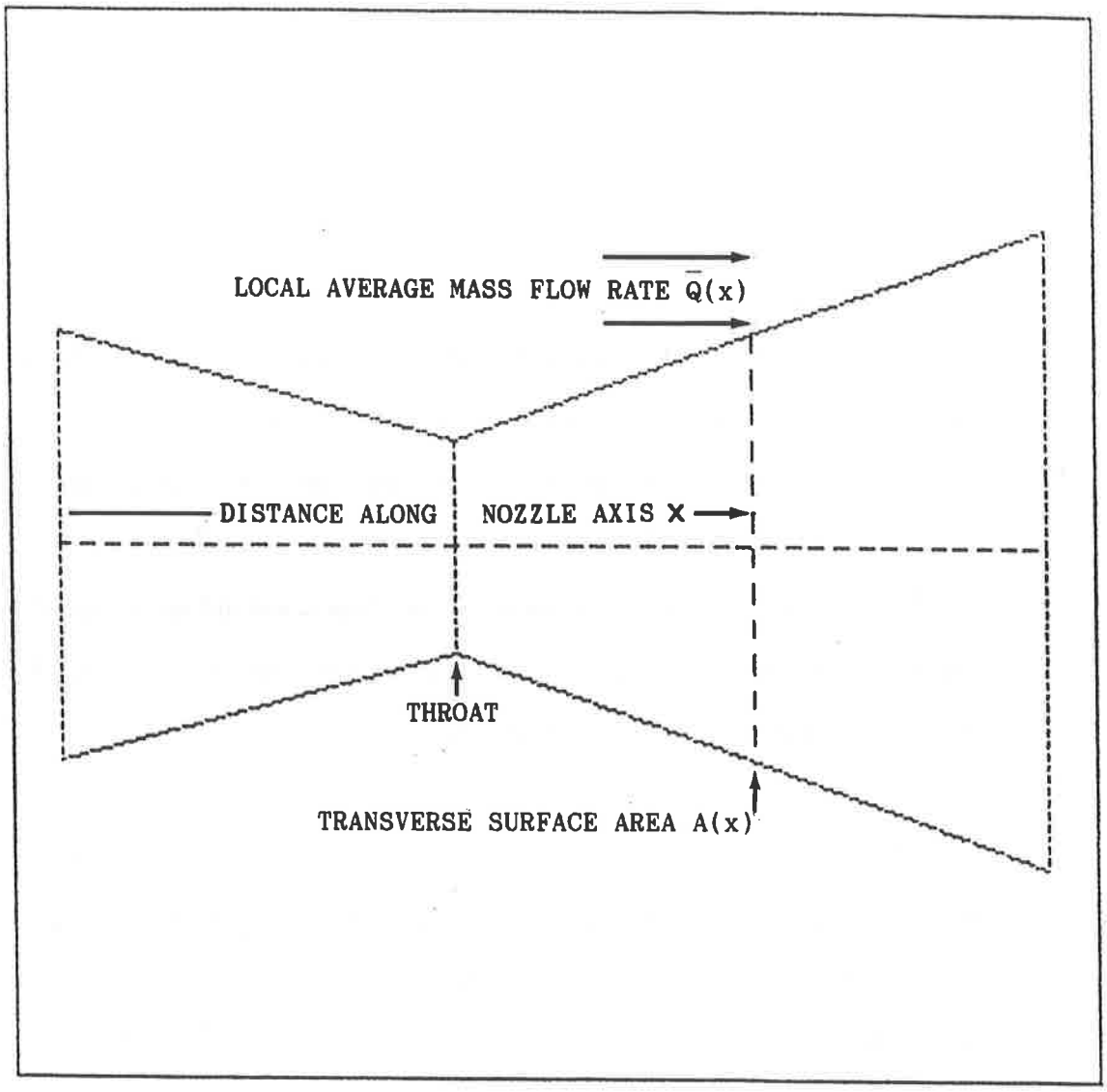

FIG FOUR

Reduction to a single streamline

The key factor in the reduction process is that it can be shown that at any arbitrary point, x, along the duct axis there exists a co-axial ring of streamlines in the flow field, through the local transverse surface, on which the mass flow rate, Q(x), equals the local average value.

The particle motion on this ring is therefore representative of the full duct flow. Although the total energy will remain constant on each streamline individually passing through the ring (from (1.15)) it may vary transversely in accordance with the specification of the total energy as a function of position across the entry surface; under these circumstances there is therefore vorticity in the flow. To allow a further reduction to a single flow representative streamline it is necessary to assume homenergicity (constant energy in the flow field) and thus irrotationality of the flow.

These assumptions are reasonable as long as the duct area variation is small. The flow under consideration can now be thought of as a primary flow through the duct and therefore the transverse surface, A(x), may be taken to be the local duct cross-sectional area. The co-axial ring of streamlines can be represented by to a single streamline defined by the constant values of total entropy and energy inherent from the homentropic and now homenergic nature of the flow.

The constant C in (2.3) can now be identified with the entry value

of mass flow rate on the typical streamline. Furthermore the motion equation (2.2) takes the particular form,

$$\frac{d\ (Q\ A)}{dx} = 0\ , \tag{2.5}$$

and the relationship,

$$Q(x) = \frac{C\ A_e}{A(x)}\ , \tag{2.6}$$

represents a local map, valid on this representative streamline, between distance along the duct axis and mass flow rate through the duct.

The complete definition of a particular motion is obtained by inclusion of the quasi one-dimensional boundary conditions. The boundaries can be thought of as a pair of points at the inlet and outlet locations on the typical streamline. The inlet boundary condition, analagous to the full duct flow (§2.1), is to specify the entry mass flow rate on that streamline,

$$Q_e = C\ . \tag{2.7}$$

The corresponding mass flow rate outlet boundary condition, Q_o, is available through implementation of the local map (2.6),

$$Q_o = \frac{C\ A_e}{A(x)}\ , \qquad (2.8)$$

where A_o is the outlet transverse surface area.

Thus in summary the concept of primary duct flow can be reduced to the consideration of particle motion on a single representative streamline defined by the constant values of entropy and total energy inherent in the definition of the flow.

SECTION THREE : FLOW VARIABLE RELATIONSHIPS FOR PRIMARY DUCT FLOW

The essential result from the derivation of the algebraic relations between the mechanical flow variables associated with a fluid particle moving on a specified streamline, and thus also in the graphical representation, is that these apply to any such motion of the particle in any flow field.

Therefore, in particular, for reduction of primary duct flow to consideration of particle motion on a single representative streamline, the algebraic relations hold. The graphical representation of these relations for this motion, and hence for the actual approximation to duct flow, may therefore be obtained. These manifest as segments of each of the set of full graphs associated with motion on a general streamline when the entropy and total energy values that are inherent in the homentropic and homenergic nature of the flow are specified; the actual values assigned are those stated previously in (1.30) and (1.31). This was considered briefly in [3] but only in relation to the de-Laval nozzle flow; the following discussion includes and expands this work.

3.1 CONE SECTION FLOW

The geometries of the cone sections considered are illustrated in FIG.3*i*,*ii*. The factors in obtaining the appropriate part of each graph, that provide the inter-variable relationships for a particular cone section motion, are the quasi one-dimensional mass flow rate boundary conditions on the representative streamline, (2.7) and (2.8).

The process of positioning ordinates at these boundary values, on the subset of the general graphs (FIGS.1,2) involving mass flow rate as a dependent variable, picks out, on each, the relationship between mass flow rate and each dependent variable throughout the complete motion. In the present case this is the portion interior to the two boundary ordinates (see FIG.5).

The subsequent availability of the boundary values of all of the flow variables, for a particular motion, allows the determination of the complete set of inter-variable relations (see FIG.6).

However the assignment of the mass flow boundary conditions for a particular cone section flow does not uniquely determine the flow type that may subsequently occur. It is equally probable that this may be one of either subsonic or supersonic flow throughout; specifying one of the associated flow inlet pressures will determine which will take place. An ordinate, denoted 'C', placed on FIG.5*iii* at the inlet mass flow rate boundary condition, for the particular motion, provides the pressure value corresponding to subsonic flow (see 'i' on FIG.5*iii*) and to

supersonic flow (see 'ii' on FIG.5*iii*). The role of the critical speed (1.33) on the streamline in distinguishing the flow types is apparent from FIG.5*i*. Additionally the effect that the section geometry has on the fluid itself is also clearly illustrated by the relationship between density and mass flow rate shown in FIG.5*ii*. It can be seen that in a converging cone section subsonic flow is expanded whereas supersonic flow is compressed, the reverse occuring in a diverging section.

Conditions for flow

The most significant flow variable value on the streamline in this context is that of mass flow rate (1.34d) which may be used to derive conditions under which a flow will occur. This critical mass flow rate value is the maximum that may occur on the streamline specified by (1.30) and (1.31) and thus the maximum value that may occur for flow through any duct modelled by the quasi one-dimensional approximation, in particular here a cone section. Through the local map (2.6) there then exists, for a cone section, a corresponding critical minimum cross-sectional area,

$$A_* = \frac{C\, A_e}{Q_*} , \qquad (3.1)$$

through which a flow may take place.

In a converging cone section on attainment of this value the flow will theoretically halt [1].

Thus to ensure flow throughout the section the entry mass flow rate to the representative streamline must be chosen so that it satisfies the condition

$$\text{FOR FLOW THROUGH A CONVERGING SECTION} \quad : \quad C \leq \frac{A_o}{A_e} Q_* \ . \qquad (3.2)$$

Similarly the analogous condition for flow to occur at all in a diverging section is

$$\text{FOR FLOW THROUGH A DIVERGING SECTION} \quad : \quad C \leq Q_* \ . \qquad (3.3)$$

Illustration cone section motions

A converging conical section is now specified through the inlet and outlet cross-sectional areas,

$$A_e = 1.15 \ , \qquad (3.4)$$
$$A_o = 1.0 \ ,$$

and the relevant parts of the graphs between the flow variables found by the specification of the mass flow rate boundary conditions, through (2.6), and in accordance with condition (3.2),

$$C = 200.0 \ , \qquad (3.5)$$
$$Q_o = 230.0 \ .$$

Inequality (3.2), for this particular section, takes the form,

$$C \leq 214.1837 \ , \tag{3.6}$$

which is obviously satisfied by the entry boundary condition here, (3.5a).

The two possible flow types throughout this converging section are represented on FIGS.5,6 in the following manner,

$$\begin{aligned} &\text{SUBSONIC FLOW} \quad : \quad a \rightarrow b \ , \\ &\text{SUPERSONIC FLOW} \quad : \quad d \rightarrow c \ , \end{aligned} \tag{3.7}$$

where a, d, are the flow entry points and b, c are the flow outlet points for the respective flow types on each graph, and the arrow indicates the variable variation in the flow direction; the critical point is indicated on each graph by '×'.

A diverging section is also specified by

$$\begin{aligned} A_e &= 1.0 \ , \\ A_o &= 1.15 \ , \end{aligned} \tag{3.8}$$

and the boundary conditions assigned through (2.6), whilst ensuring that condition (3.3) is upheld, by

$$C = 230.0$$

and (3.9)

$$Q_o = 200.0 \ .$$

The relationships between the flow variables for the two possible flow types throughout the diverging section are again shown on FIGS.5,6, and explained below, in which the notation takes the same meaning as previously,

SUBSONIC FLOW : $b \rightarrow a$,

and (3.10)

SUPERSONIC FLOW : $c \rightarrow d$.

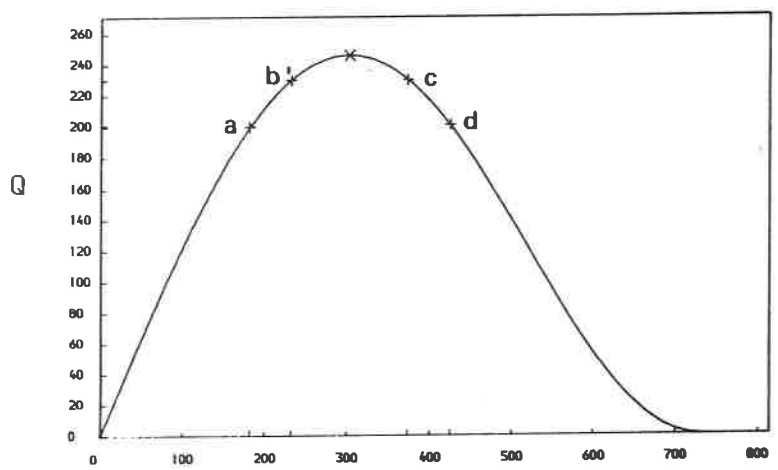

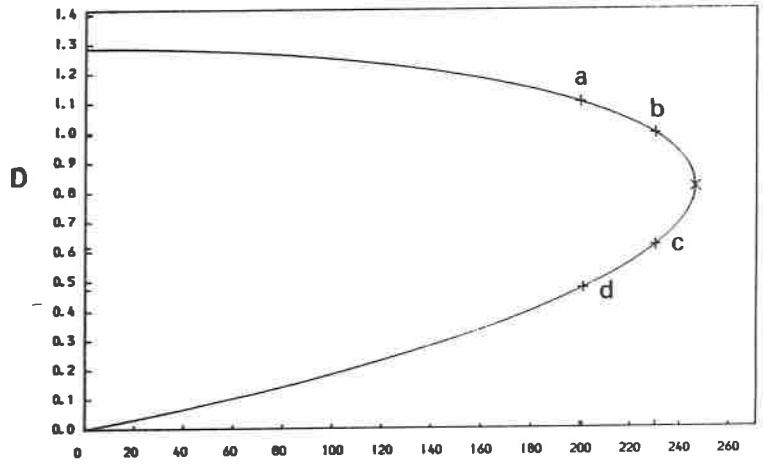

SECTION FLOW VARIABLE VARIATION WITH RESPECT TO MASS FLOW RATE

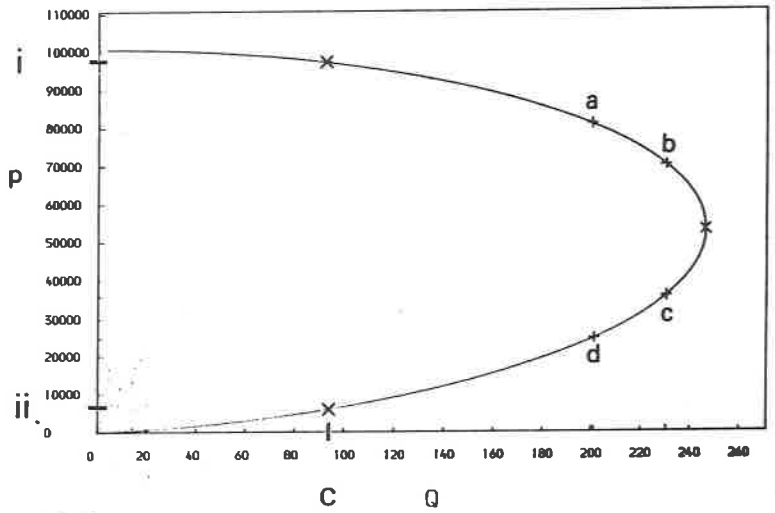

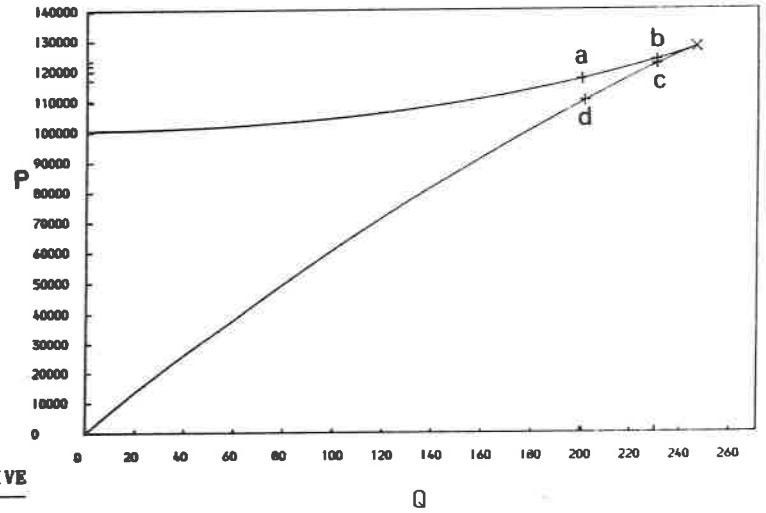

FIG. FIVE

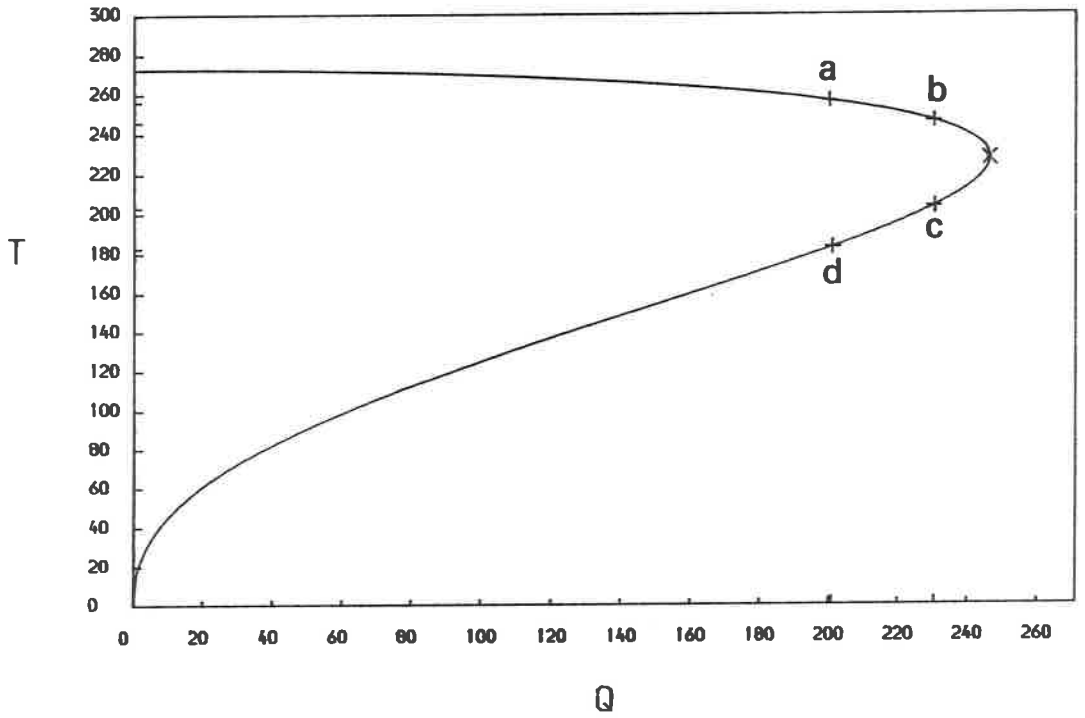

FIG. FIVE

cont.

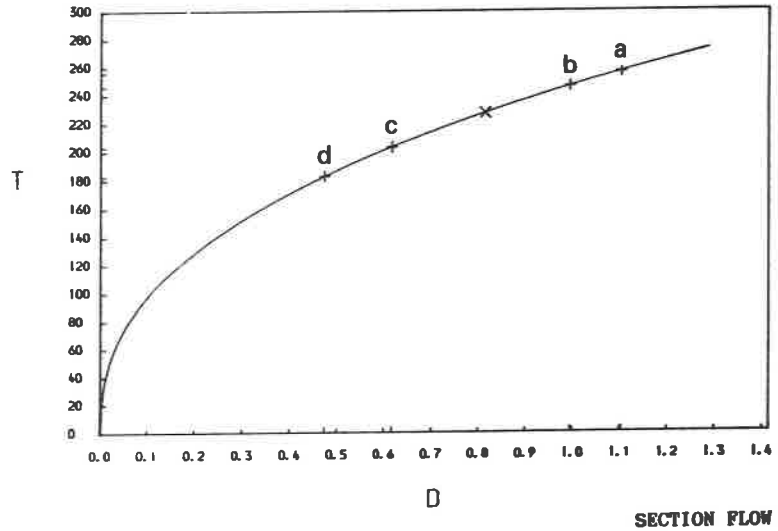

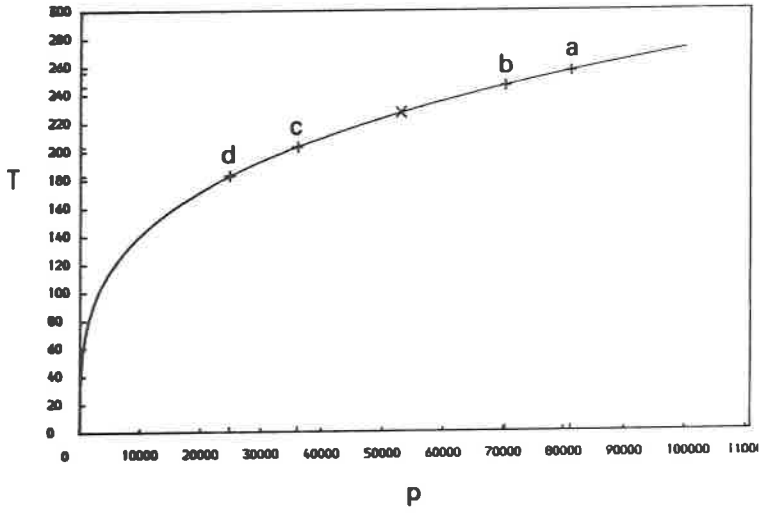

SECTION FLOW VARIABLE INTER-RELATION

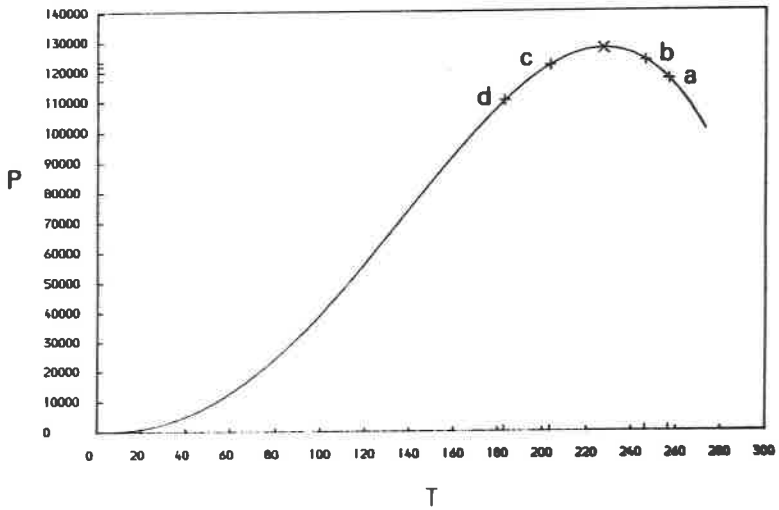

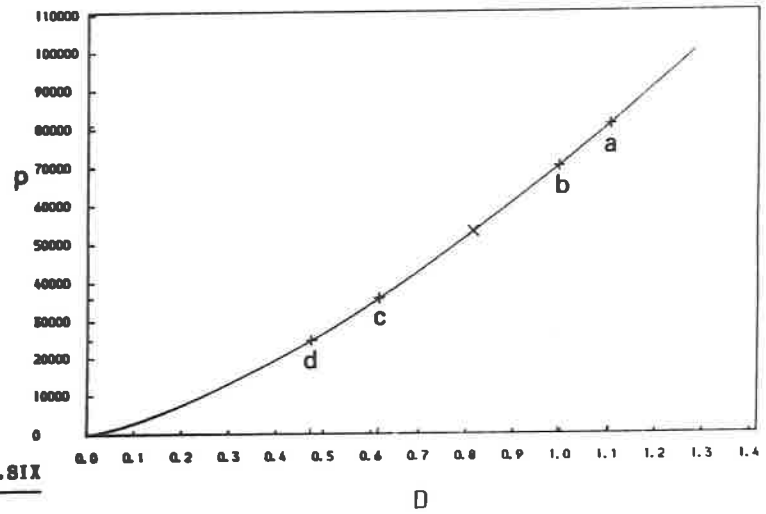

FIG.SIX

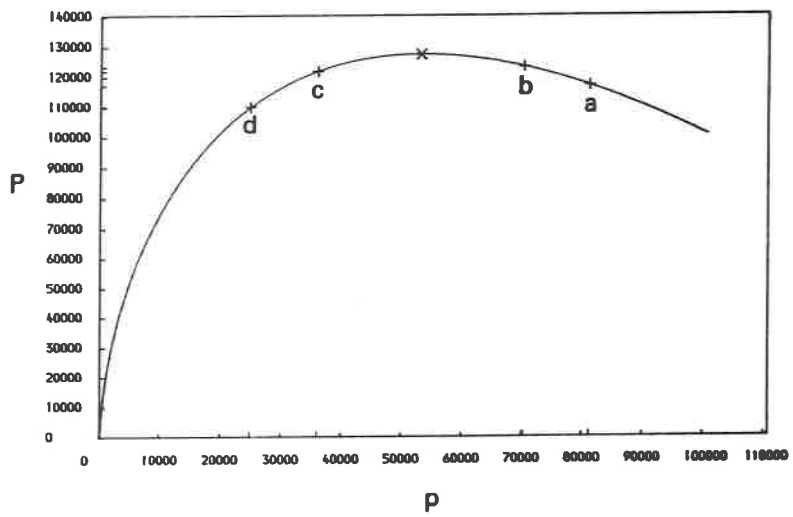

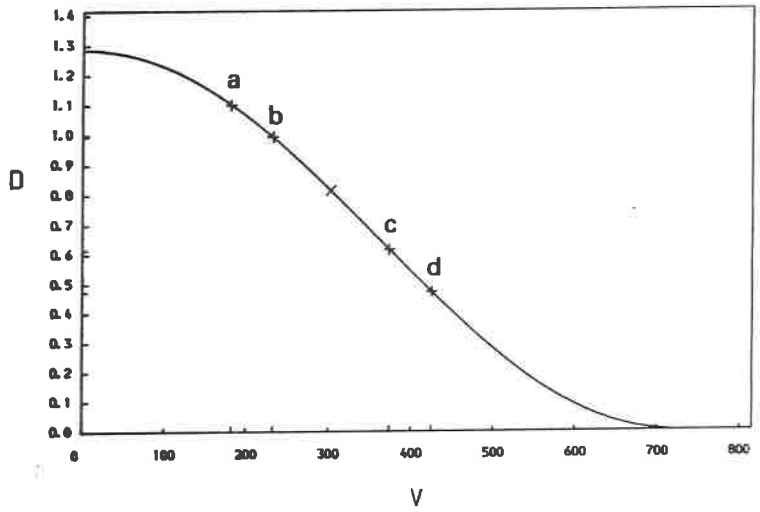

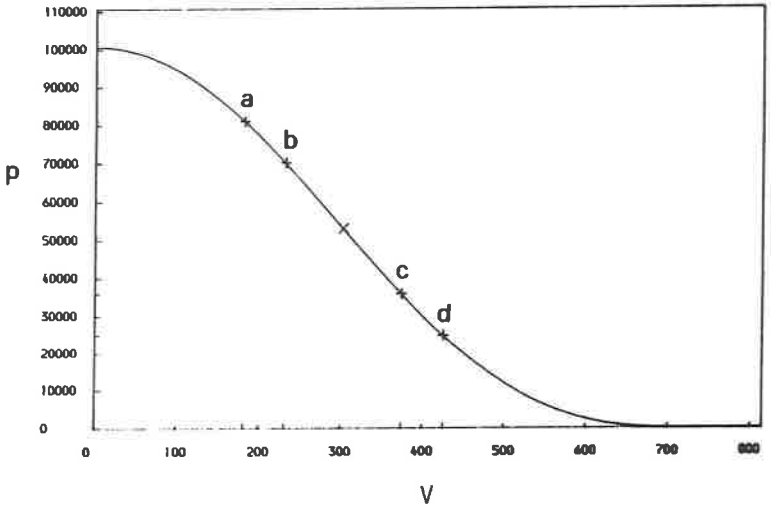

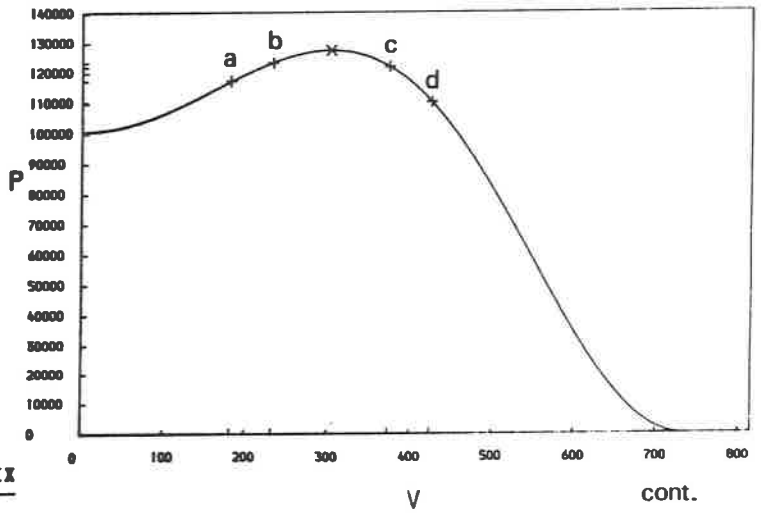

FIG.SIX

cont.

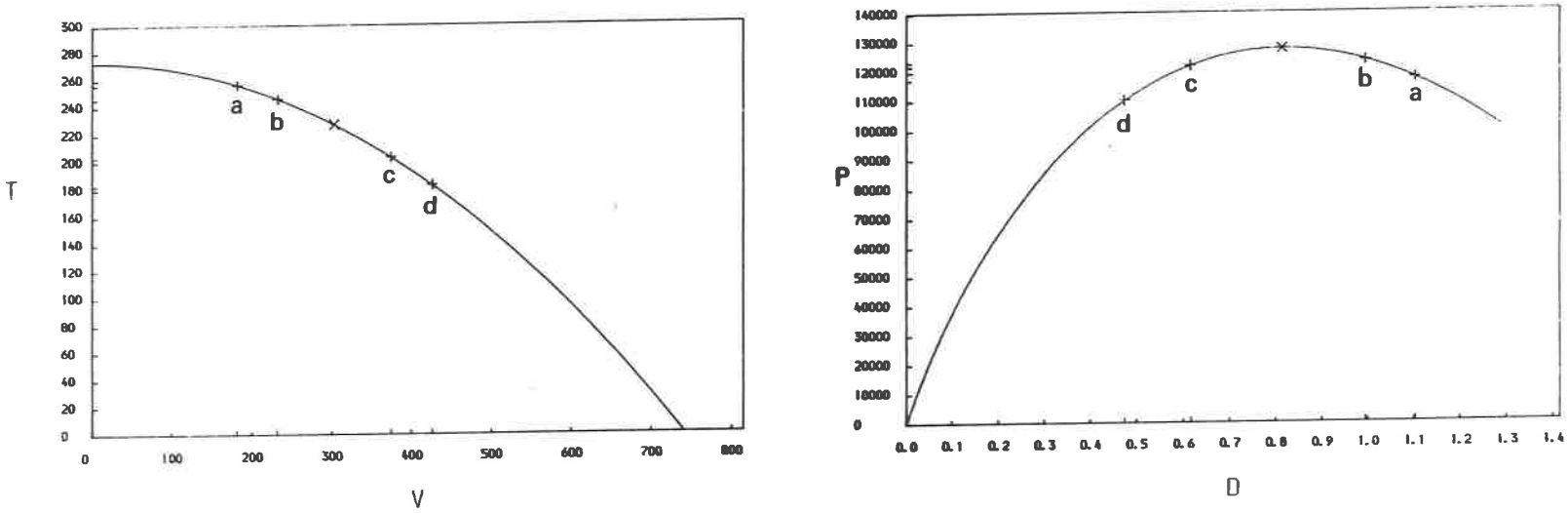

FIG.SIX

cont.

3.2 DE-LAVAL NOZZLE FLOW

The relationships between variables for the flow through a specified de-Laval nozzle, of the form (FIG.3*iii*), are obtained by fundamentally the same process that was employed for cone section flow. An additional factor arises though, due to the existence of the single cross-section of minimum area, A_t, at the nozzle throat. The maximum mass flow rate, Q_t,that can possibly occur throughout a particular nozzle can then be obtained directly from the local map (2.6), and is given by,

$$Q_t = \frac{C.A_e}{A_t} \quad . \tag{3.11}$$

Thus for a particular nozzle motion the relation paths are now determined by a triplet of ordinates placed on FIGS.1,2, at the associated boundary and throat mass flow rate values (2.7), (2.8) and (3.11); the flow trajectory will pass through these, as explained below, dependent on the flow behaviour throughout the nozzle (see FIGS.8,9).

Flow behaviour

The important condition in the determination of this behaviour concerns the maximum throat mass flow rate (3.11) in comparison with the critical value (1.34d). On making the assumption that the fluid enters the nozzle subsonically (1.20a), only a finite number of possibilities may subsequently occur.

To clarify the discussion an illustrative path, relating flow stress and mass flow rate, associated with each of the flows is provided in FIG.7. Note the critical values on each graph dividing the relation into regions of subsonic and supersonic flow.

1. Subsonic flow

If the mass flow rate at the throat is less than the critical value then the flow will remain subsonic throughout the complete nozzle,

$$Q_t < Q_* \ . \tag{3.12}$$

There then exists a single path, remaining on the subsonic segment, on each of FIGS.1,2; this occurs in two distinct stages reversing at the throat ordinate, which is shown below with reference to FIG.7*ii*,

$$a \rightarrow c \rightarrow b \ , \tag{3.13}$$

where 'a' corresponds to the nozzle entry point, 'b' to the subsonic outlet point and 'c' to the critical point. The particular flow variable behaviour for this illustrative case is given below, noting that P_e, P_t and P_o^{sub} are the inlet, throat and subsonic outlet values of flow stress respectively.

$$\begin{aligned} &C \rightarrow Q_t \rightarrow Q_o \ , \\ &P_e \rightarrow P_t \rightarrow P_o^{sub} \ . \end{aligned} \tag{3.14}$$

2. Terminating flow

This flow behaviour results if the mass flow rate at the throat potentially exceeds the critical value, i.e.

$$Q_t > Q_* \ . \tag{3.15}$$

This maximum mass flow rate will actually then occur at the location in the nozzle entry section where

$$A(x) = A_* = \frac{C\,A_e}{Q_*} \ , \tag{3.16}$$

and it is at this point that the flow will theoretically halt (see [1]). The predicted value at the throat cannot exist and the nozzle is said to be choked. This is similar to the occurrence in cone flow where in the present case the throat cross-sectional area is less than the critical value (3.1) associated with that particular motion and therefore in the same way conditions can be derived here which will be necessary if flow is to occur. Flow throughout the complete nozzle can be ensured by specifying the inlet boundary condition in accordance with the condition,

$$C \leq \frac{A_t\,Q_*}{A_e} \ . \tag{3.17}$$

In this case the path representing the inter-variable relationship

on each of the graphs FIGS.1,2 will then terminate at the respective critical values, in the case of FIG.7*iii* shown below, where 'a' is the duct inlet point and 'e' is the critical point past which the flow cannot occur,

$$a \rightarrow e \ . \tag{3.18}$$

This can also be seen in terms of the actual flow variables present in FIG.7*iii*,

$$\begin{aligned} C &\rightarrow Q_* \ , \\ P_e &\rightarrow P_* \ , \end{aligned} \tag{3.19}$$

where P_* is the critical value of flow stress.

3. Transition flow

On the actual equality of the throat mass flow rate with the critical value,

$$Q_t = Q_* \ , \tag{3.20}$$

and therefore on coincidence of the throat area with that critical value associated with the particular motion (3.1), one of two possible flow types may arise in the nozzle exhaust section.

The first possibility is that the flow will remain subsonic throughout the nozzle taking the critical flow variable values at the throat, e.g. as here,

$$\begin{aligned} C &\rightarrow Q_* \rightarrow Q_o \ , \\ P_e &\rightarrow P_* \rightarrow P_o^{sub} \ , \end{aligned} \tag{3.21}$$

and thus the relation path will remain on the subsonic segment, where with reference to FIG.7d (a, b, c, take the same meaning as previously)

$$a \rightarrow c \rightarrow b \ . \tag{3.22}$$

Alternatively under the correct conditions it may become 'sonic at the throat' and subsequently supersonic in the diffuser. The associated path on the graphs will now continue through the respective critical values and onto the supersonic segment, i.e. with respect to FIG.7*iv*,

$$a \rightarrow c \rightarrow d \ , \tag{3.23}$$

where d is the supersonic outlet point and, with respect to the actual flow variables being considered in this illustration,

$$\begin{aligned} C &\rightarrow Q_* \rightarrow Q_o \ , \\ P_e &\rightarrow P_* \rightarrow P_o^{sup} , \end{aligned} \tag{3.24}$$

where P_o^{sup} is the supersonic outlet value of flow stress.

The conditions necessary for the latter to occur are directly related to the outlet pressure of the nozzle. Inspection of FIG.7a, with an ordinate erected at the outlet mass flow boundary condition for the particular motion, gives two alternative choices of this quantity, indicated thereon by 'b' and 'd'. If neither of these are enforced the flow will remain subsonic throughout the nozzle, but prescription of either of these values will determine directly the nature of the corresponding diffuser flow,

$$p_o^{sub} \quad (b) \quad : \quad \text{SUBSONIC DIFFUSER FLOW} \,, \qquad (3.25)$$

$$p_o^{sup} \quad (d) \quad : \quad \text{SUPERSONIC DIFFUSER FLOW} \,.$$

The split of a solution, at a defined point, into two that are equally probable is termed a bifurcation, which in the present case occurs at the sonic point.

Therefore the significant difference between section flow and de-Laval nozzle flow is the possibility of a transition from subsonic to supersonic flow at the nozzle throat. This can take place at no other location because attainment of the critical mass flow rate (1.34d) must occur where the nozzle area is critical, by (3.1), and if this did not occur at the throat then the flow would terminate.

The inlet boundary condition must be adjusted to allow transition

flow through the equality of (3.17), the condition becoming

$$C = \frac{Q_*}{A_e} \frac{A_t}{} \quad . \tag{3.26}$$

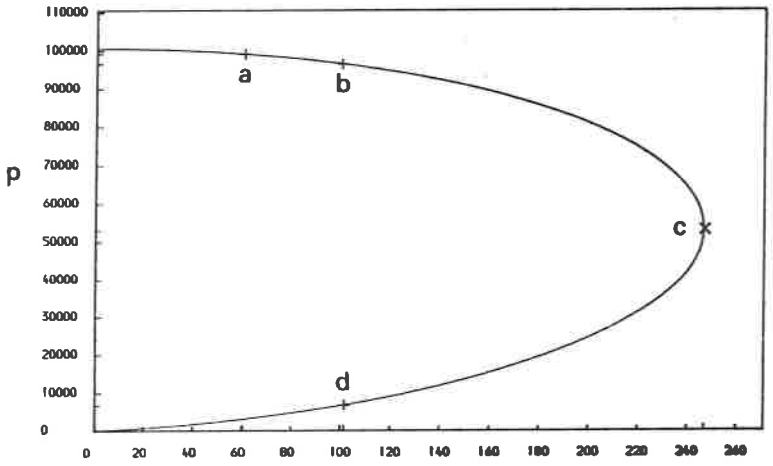

DEFINITIVE OUTLET PRESSURES

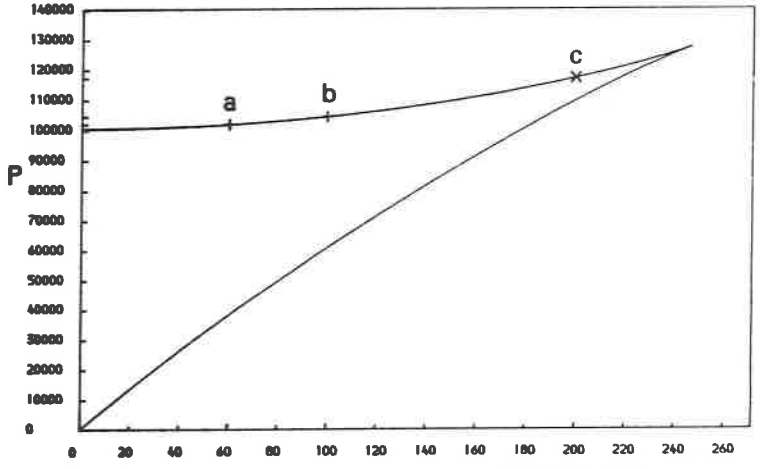

SUBSONIC FLOW

NOZZLE FLOW BEHAVIOUR

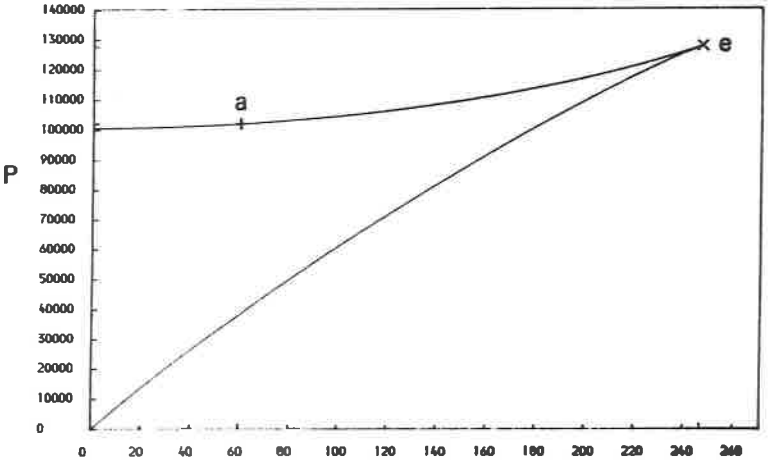

TERMINATING FLOW

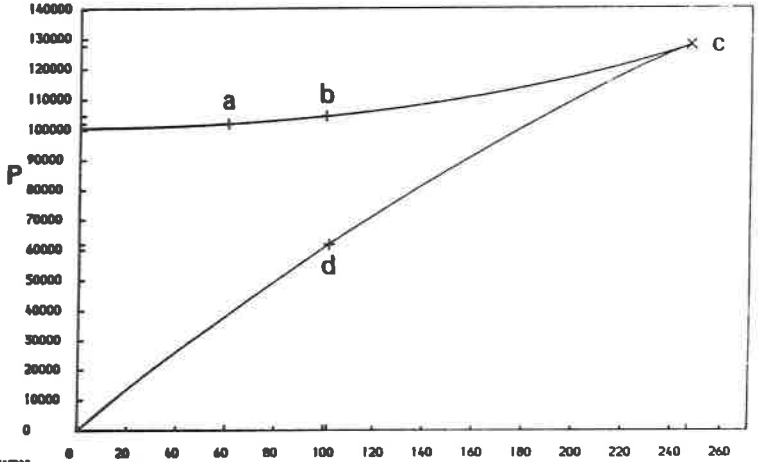

TRANSITION FLOW

FIG SEVEN

Illustration of a nozzle motion

An illustration of the de-Laval nozzle is given by specifying the inlet, outlet and throat cross-sectional areas such that the minimum area occurs at the throat. We can take as an example,

$$A_e = 1.1 \ ,$$
$$A_t = 1.0 \ , \qquad (3.27)$$
and $$A_o = 1.2 \ .$$

The relationships between flow variables for subsonic flow throughout, critical at the throat, and transition flow are then obtained by specification of the mass flow rate triplet (2.7), (2.8) and (3.11); these are assigned below through the local map (2.6) and are chosen such that the transition flow condition (3.26) holds

$$C = 223.9193 \ ,$$
$$Q_t = Q_* = 246.31124 \ , \qquad (3.28)$$
$$Q_o = 205.25936 \ .$$

The variation of each flow variable with respect to mass flow rate throughout the nozzle is shown in FIG.8 and subsequently the inter-variation for the remaining pairs of variables in FIG.9. In both of these set of graphs the two possible flow behaviours are indicated in the following way

$$a \rightarrow c \rightarrow b \quad : \quad \text{SUBSONIC FLOW} \,, \tag{3.29}$$

$$a \rightarrow c \rightarrow d \quad : \quad \text{TRANSITION FLOW} \,,$$

where 'a' is the respective variable inlet value, 'b' the subsonic outlet value, 'd' the supersonic outlet value and 'c' the critical point.

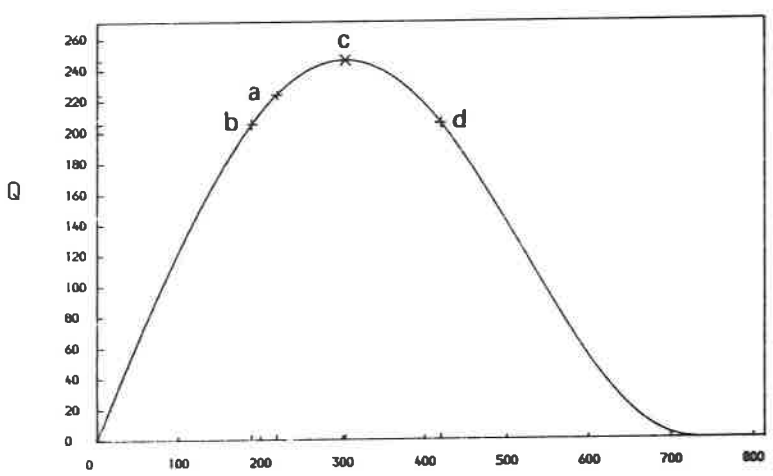

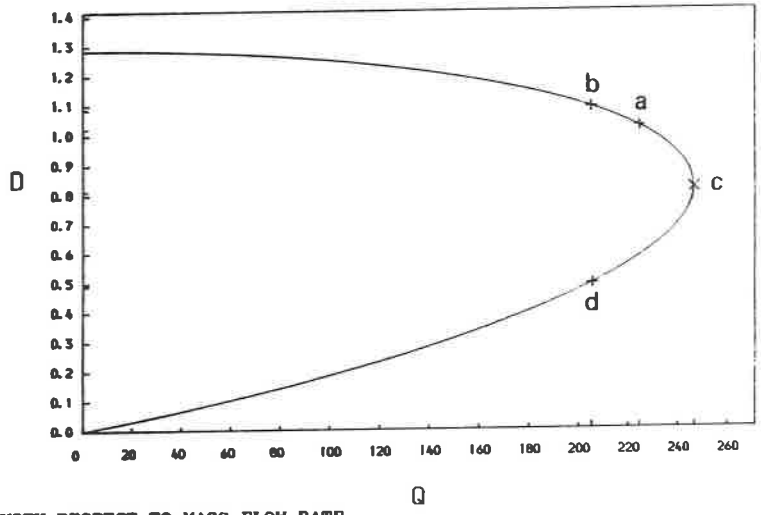

NOZZLE FLOW VARIABLE VARIATION WITH RESPECT TO MASS FLOW RATE

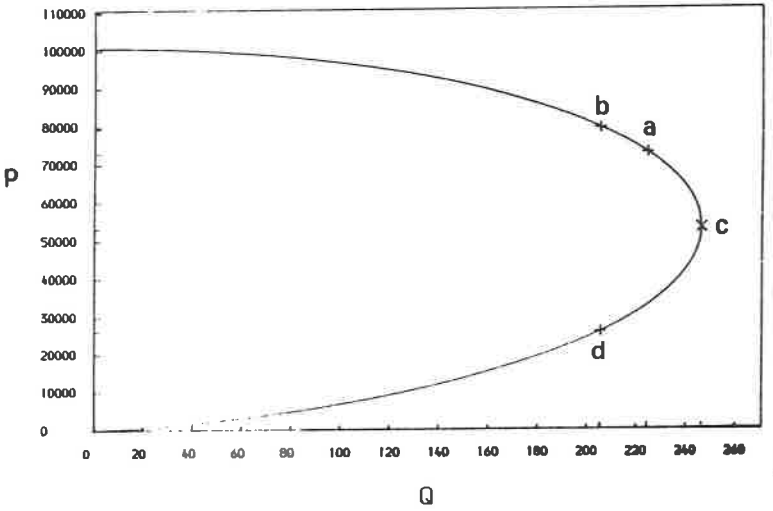

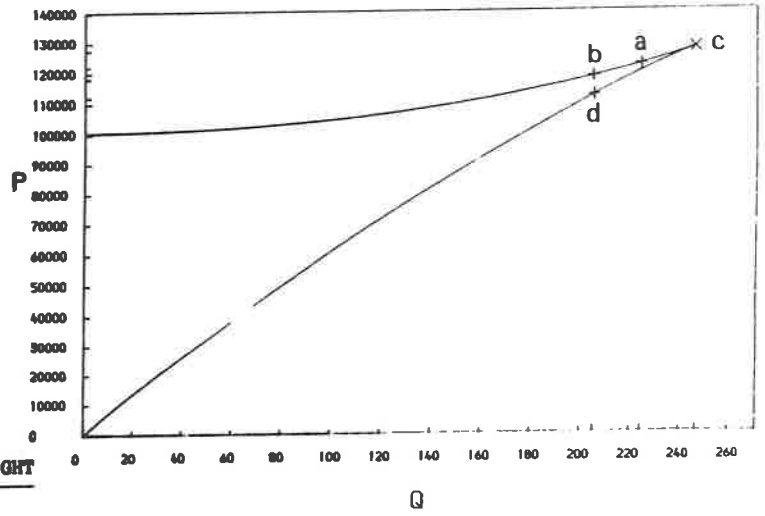

FIG EIGHT

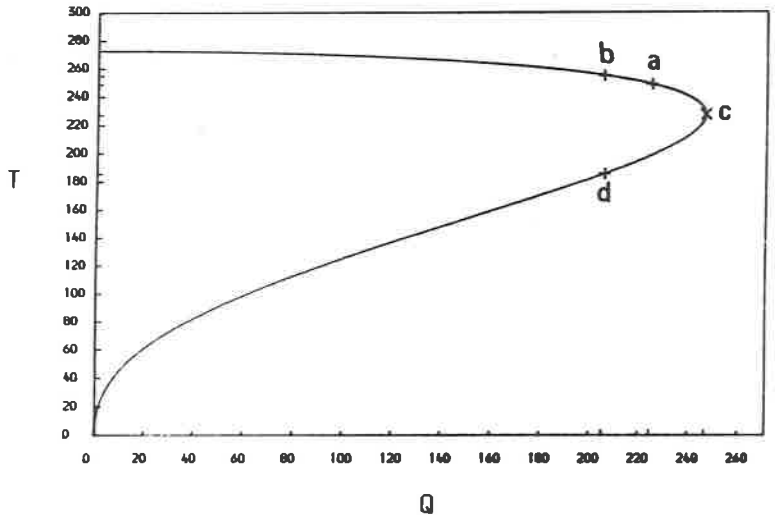

FIG EIGHT

cont.

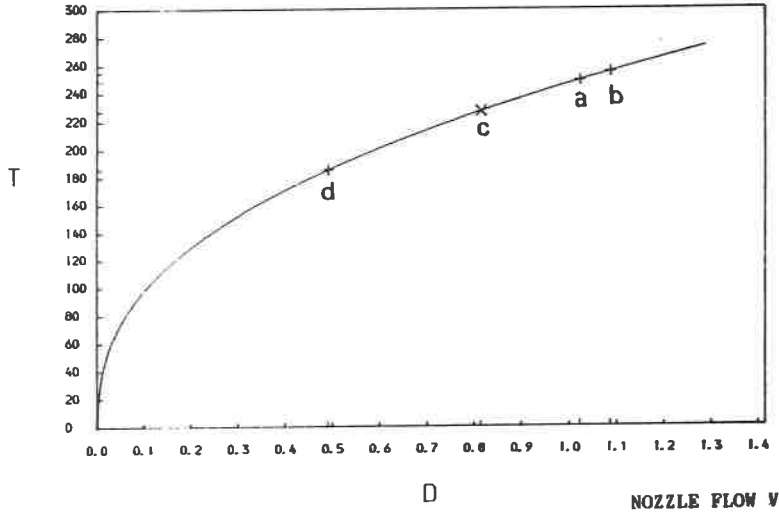

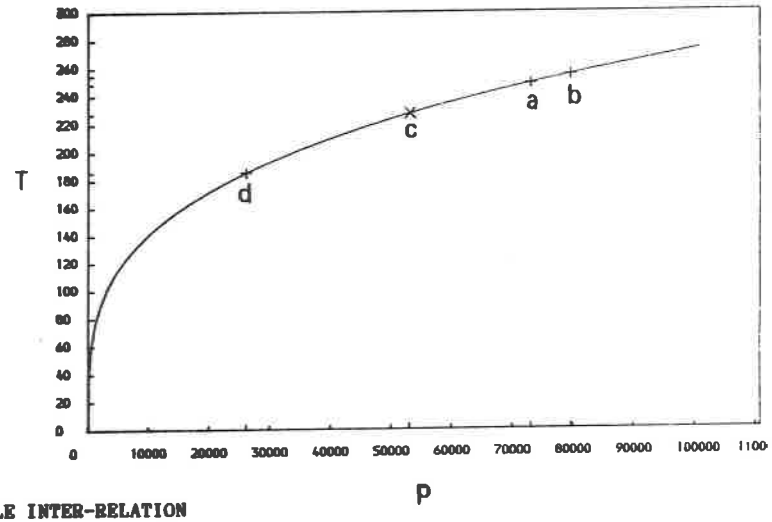

NOZZLE FLOW VARIABLE INTER-RELATION

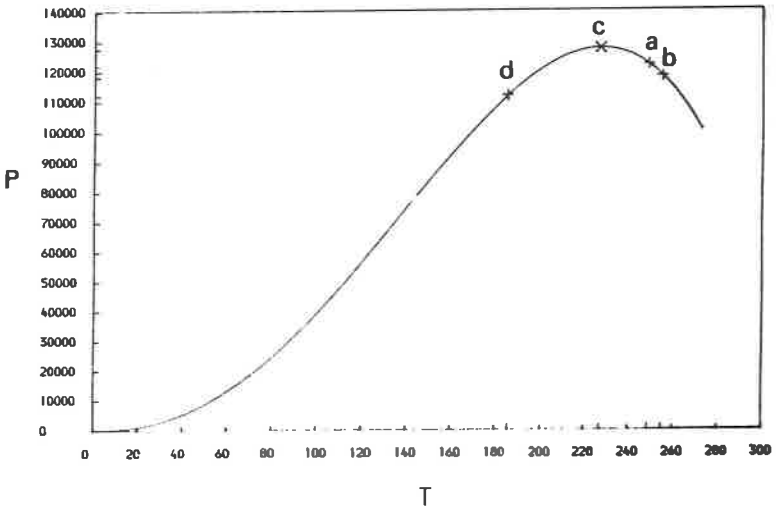

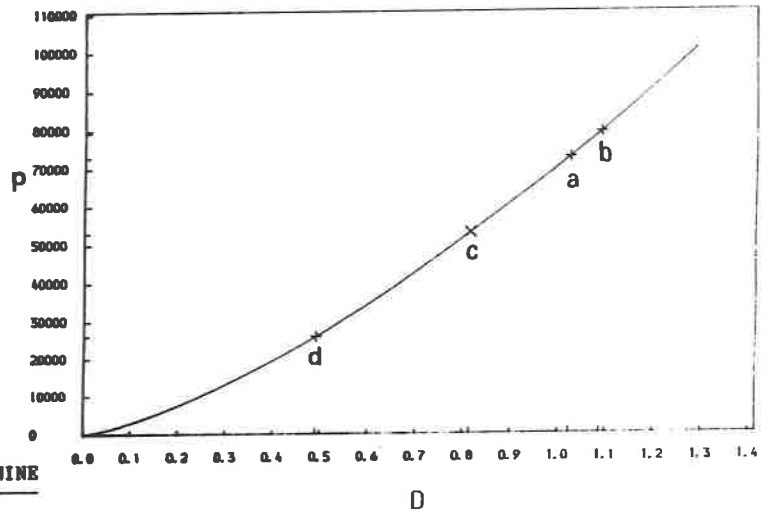

FIG NINE

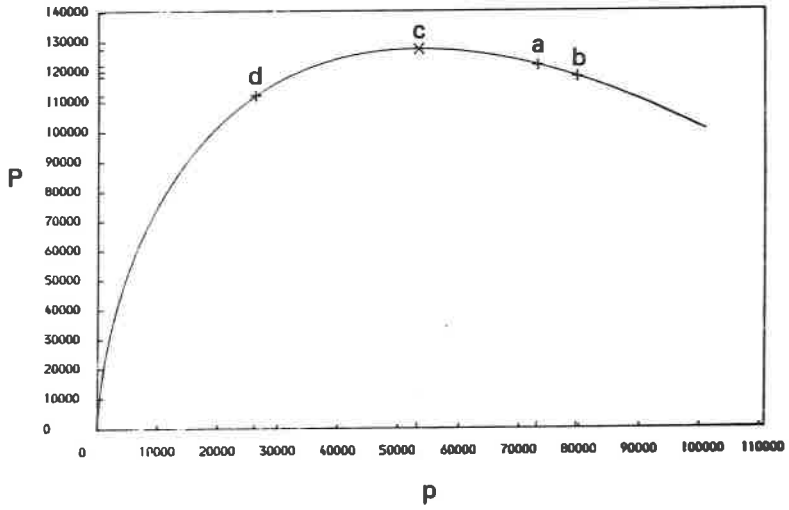

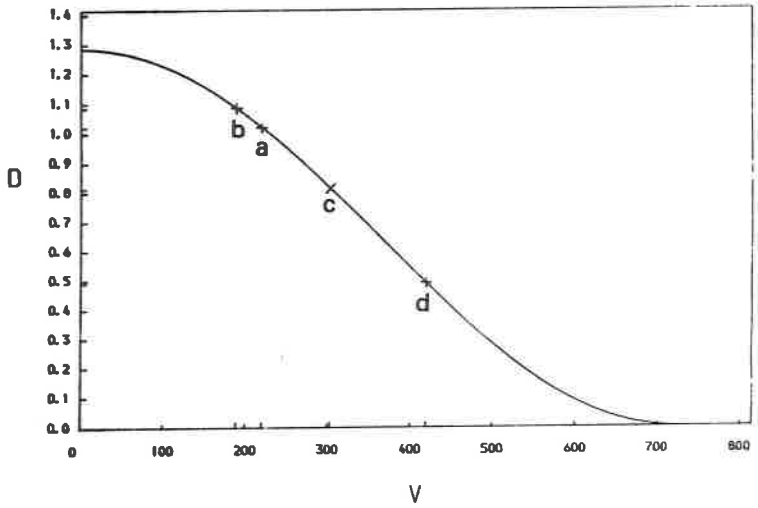

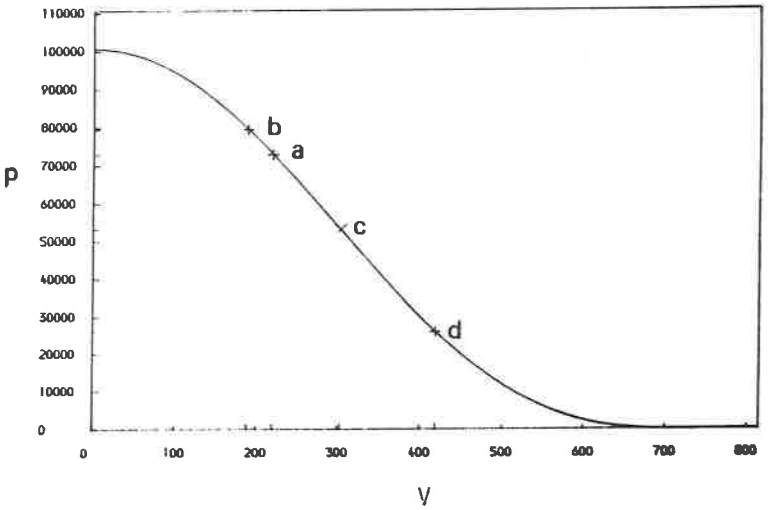

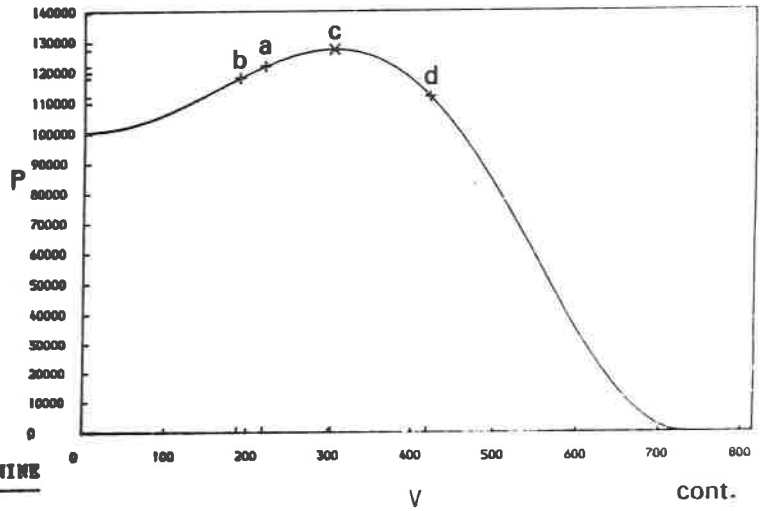

FIG NINE

cont.

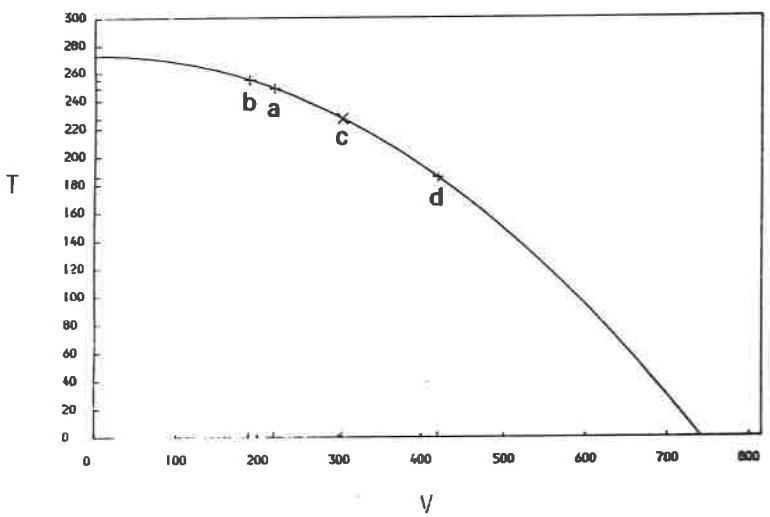

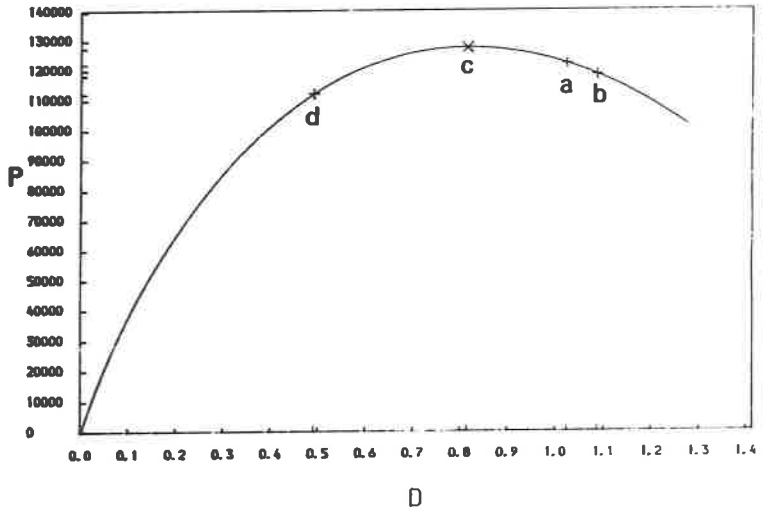

FIG NINE

cont.

SECTION FOUR : AN ALGEBRAIC FORMULATION FOR PRIMARY DUCT FLOW

The aim of the concluding section of this report is to determine the specific variation of each flow variable, for a particular motion, in terms of the spatial distance, x, used as a parameter along the duct axis. This will provide an exact solution preceding a finite element approximation of primary duct flow to follow in a subsequent report.

The graphical representation of the algebraic relations between the flow variables for a particle moving on the duct typical streamline contains the variable inter-relation throughout the duct itself; thus this parameterization can be used in obtaining the required variation of each variable with x.

On specification of a range of spatial locations between the duct inlet and outlet stations, i.e. distances along the duct axis, the local map on the streamline (2.6) gives the corresponding axial mass flow rate variation, lying between the associated boundary values (2.7) and (2.8), for that motion. The corresponding ordinates at these values on the subset of graphs (FIGS.1,2), involving mass flow rate as a dependent variable, then provides, by inspection, the axial variation of the each of the other flow variables. This is indicated schematically as

$$x \;\rightarrow\; \underset{[2.6]}{Q(X)} \;\rightarrow\; \underset{(FIGS.1,2)}{v(x),p(x),\rho(x),T(x),P(x)}\ . \qquad (4.1)$$

This process, although theoretically correct, is inefficient to implement. The method actually used to determine the flow variable axial variation is a particular extension, applicable to quasi one-dimensional duct flow, of that used for the derivation of the algebraic relations associated with particle motion on a general streamline (§1), now applied to the motion on the duct representative streamline.

4.1 FORMULATION

The theory associated with particle motion on a specified general streamline (§1) shows that Bernouilli's equation (1.15) holds thereon in the flow field. This streamline is chosen to be the representative streamline in the context of quasi one-dimensional duct flow and the constant entropy and total energy values assigned to be those inherent from the properties of the full flow, i.e. (1.30) and (1.31).

Substitution of the equation of state for the gas medium (1.5) and the expression for the internal energy (1.7) into (1.15) may yield, if rearranged in an alternative manner to (1.18), a relation between density and fluid speed, namely,

$$v^2 + 2\,\eta \left[\frac{\gamma}{\gamma-1} \right] \rho^{\gamma-1} = 2\,h\,. \qquad (4.2)$$

A second such relationship between these two flow variables is obtained by rearrangement of (2.6) and substitution of (1.16) to give

$$\rho(v) = \frac{C\ A_e}{v\ A(x)} \tag{4.3}$$

where the assumption has been made, consistent with primary duct flow, that the duct area variation is small,

$$\frac{dA}{dx} < \delta \ . \tag{4.4}$$

Substitution of (4.3) into (4.2) then provides an explicit non-linear relationship between the duct axial location and the local fluid speed on the representative streamline,

$$v^2 + 2\ \eta \left[\frac{\gamma}{\gamma-1} \right] \left[\frac{C\ A_e}{v\ A(x)} \right]^{\gamma-1} = 2\ h\ v^{\gamma-1} \ , \tag{4.5}$$

and more specifically in the present case for air flow by,

$$v^2 + 7\ \eta \left[\frac{C\ A_e}{v\ A(x)} \right]^{0.4} = 2\ h\ v^{0.4} \ . \tag{4.6}$$

A relationship unique to a particular motion may be obtained through substitution of the flow constants (1.30), (1.31) and specification of the duct area variation, together with the mass flow rate entry condition (2.7).

4.2 SOLUTION ALGORITHM FOR DUCT RELATION

The fluid speed, at an arbitrary spatial position in the duct, on the representative streamline, is computed by the application of a fixed point iterative algorithm on the rearranged form of (4.6),

$$F(v) \equiv v^2 - 2\,h\,v^{0.4} + 7\,\eta \left[\frac{C\,A_e}{v\,A(x)} \right]^{0.4} = 0 \ . \qquad (4.7)$$

A general iterative algorithm is first considered,

$$v^{i+1} = g(v^i) \ , \qquad (4.8)$$

defined such that at the root, v_*,

$$v_* = g(v_*) \ , \qquad (4.9)$$

where v^{i+1} is the updated solution at iteration level i+1 and v^i is the solution at the present iteration level i.

A sequence of root approximations $\{ v^i \}$ (at iteration level i) is generated by the iterative scheme (4.8) commencing at an initial value v^o. Then from (4.8) and (4.9),

$$v^{i+1} - v_* = g(v^i) - g(v_*) \ . \qquad (4.10)$$

Then by the Mean Value Theorem [4], if (4.8) is continuous and

differentiable on an interval [a,b], then

$$(v^{i+1} - v_*) \leq (v^i - v_*) \, g'(\xi) \, , \tag{4.11}$$

where $v^i < \xi < v_*$. The iterative scheme defined by (4.8) will then converge in a region around the root if

$$| g' | < 1 \tag{4.12}$$

which implies from (4.11) that

$$| v^{i+1} - v_* | < | v^i - v_* | \tag{4.13}$$

and hence that

$$\lim_{i \to \infty} (v^{i+1}) = v_* \, . \tag{4.14}$$

The particular iterative algorithm we shall employ in the solution of the equation (4.7) is Newton's single variable method expressed through a particular right hand side of (4.8),

$$g(v^i) = v^i - \left[F(v^i)/F'(v^i) \right] \tag{4.15}$$

where $F'(v^i) = 2 \, v^i - 0.8 \, h \, (v^i)^{-1.6}$, (4.16)

with ' ' ' indicating the first derivative with respect to the function argument and

$$F''(v^i) = 2 + 1.28\ h\ (v^i)^{-2.6}\ , \qquad (4.17)$$

with ' " ' indicating the second derivative with respect to the function argument.

Now, as required for the Mean Value Theorem, the function g in (4.15) is continuous and differentiable on [a,b] and therefore Newton's method will converge in a region around the root if the convergence condition (4.12) holds. In the present case, from (4.15), this takes the form

$$\left| \frac{F(v^i)\ F''(v^i)}{[\ F'(v^i)]^2} \right| < 1\ . \qquad (4.18)$$

In the context of quasi one-dimensional duct flow, by substitution of the relation (4.7) and its derivatives (4.16) and (4.17), the modulus term in (4.18) will take the particular form

$$\left| \frac{\left[\ [v^i]^2 - 2\ h\ [v^i]^{0.4} + 7\ \eta\ [C\ A\ /A(x)]^{0.4}\ \right]\ \left[\ 2 + 1.28\ h\ [v^i]^{-2.6}\right]}{\left[\ 2\ [v^i] - 0.8\ [v^i]^{-1.6}\ \right]^2} \right| \qquad (4.19)$$

We now discuss quadratic convergence of Newton's scheme by considering its application to the solution of an arbitrary non-linear function.

It is necessary to make several assumptions about the function and its associated derivatives

1. THE ROOT(S) OF THE FUNCTION ARE OF MULTIPLICITY ONE ,
2. THE FIRST DERIVATIVE OF THE FUNCTION IS NON-ZERO , (4.20)
3. THE SECOND DERIVATIVE IS CONTINUOUS ,

where 2. and 3. hold in respective open interval(s) containing its root(s).

Then there exists an $\epsilon > 0$ such that the iterative algorithm is quadratically convergent to the root(s) whenever the initial data is specified such that the condition,

$$| v^{o} - v_{*} | < \epsilon , \tag{4.21}$$

holds (see [5]).

In the present case the non-linear function is (4.7) relating the fluid speed to the axial location in the duct. It has been shown for such a motion that there may exist two flow types, subsonic and supersonic, throughout; this intuitively suggests the existence of two distinct associated roots, each with multiplicity one, at each axial position.

The first derivative (4.16) of the function is non-zero for all positive values of its argument except when undefined at zero or for the

particular value

$$v^i = (0.4\ h)^{1/2.6} \cong 86.774 , \qquad (4.22)$$

while the second derivative (4.17) is continuous on $(0,\beta)$ for all values of β (see [4]).

It may be assumed that the duct axial fluid speeds will be positive, and we thus conclude that the conditions (4.20) certainly hold in open intervals (0,86) and (87,α), where now α is an arbitrary positive number.

Therefore if the zero(s) of the function F in (4.7) lie in either of these open intervals then there exists an $\epsilon > 0$ such that on application of Newton's method (4.15) to (4.7) the convergence is quadratic whenever (4.21) is upheld.

Finally convergence is assumed to have been reached when the absolute value of the residual of (4.7) is less than the specified tolerance,

$$\left| F(v^i) \right| < 0.00001 . \qquad (4.23)$$

4.3 CONE SECTION FLOW PARAMETERIZATION

The axial fluid speed variation for a particular motion is obtained by evaluating the solution of the equation (4.7) at a specified discrete number of positions throughout the cone section. The domain of solution, on which the section lies is defined as

$$0.0 \leq x \leq 1.0 \ . \tag{4.24}$$

The variation is determined firstly for flow through a converging cone section defined by (3.4) for the explicit area variation

$$A(x) = 1.0 + 0.1\ (1.0-x) + 0.05\ (1-x)^2 \tag{4.25}$$

(see FIG.10i), and then for flow through a diverging cone section specified by (3.6) and

$$A(x) = 1.0 + 0.1\ x + 0.05\ x^2 \tag{4.26}$$

(see FIG.11i).

The particular form of the non-linear relation for each of the motions are, for flow through the converging section,

$$F(v) = v^2 - 2\ h\ v^{0.4} + 7\ \eta \left[\frac{230.0}{1 + 0.1(1-x) + 0.05(1-x)^2} \right] , \tag{4.27}$$

and for flow through the diverging section,

$$F(v) = v^2 - 2\,h\,v^{0.4} + 7\,\eta\left[\frac{230.0}{1 + 0.1x + 0.05\,x^2}\right], \qquad (4.28)$$

where, recall, the flow constants are (1.30) and (1.31).

To ensure convergence of the iterative scheme applied to the solution of F = 0 in both of the above cases the initial data must satisfy the associated form of the convergence condition (4.18) [with (4.19)]. In the present case there are 101 spatial locations axially, uniformly spaced, throughout the solution domain. The bounding initial data intervals associated with a sample of these locations, for each motion (see TABLES.1,2), is used ultimately to define constant initial data over the entire solution domain; this will satisfy in each case the respective intersection bounding interval,

CONVERGING SECTION FLOW : [10,774] , (4.29)

or

DIVERGING SECTION FLOW : [10,774] . (4.30)

Note that the coincidence of these is simply a consequence of the fluid speeds throughout the two cone section motions being the inverse of each other.

CONVERGING SECTION	BOUNDING INITIAL DATA INTERVALS	
DOMAIN LOCATION x	SECTION AREA A(x)	BOUNDING INTERVAL $[\alpha,\beta]$
0.0	1.15	[9,774]
0.5	1.0625	[10,790]
1.0	1.0	[9,782]

TABLE ONE

DIVERGING SECTION	BOUNDING INITIAL DATA INTERVALS	
DOMAIN LOCATION x	SECTION AREA A(x)	BOUNDING INTERVAL $[\alpha,\beta]$
0.0	1.0	[10,790]
0.5	1.0625	[9,782]
1.0	1.15	[9,774]

TABLE TWO

Numerical experiment confirms the existence, within an arbitrary initial data bounding interval associated with an axial location, $[\alpha,\beta]$, of two distinct internal intervals,

$$[r1] \;:\; [\alpha,302.5) \;, \qquad (4.31)$$

$$[r2] \;:\; [302.5,\beta] \;,$$

the dividing factor being the critical fluid speed value (1.33).

On solution of F = 0 in either case, (4.27) or (4.28), at a specified location it would intuitively be expected that the assignment of initial data from [r1] would cause convergence of the iterative method (4.15) to the respective subsonic root and if from [r2] to the supersonic root

This division into intervals [r1] and [r2] is true of all of the bounding intervals at every position in the solution domain and therefore the initial data intersection intervals (4.29) and (4.30) for both motions can be divided globally into distinct intervals,

$$[R1] \;:\; 10.0 \leq v^{o} < 302.5 \;, \qquad (4.32)$$

$$[R2] \;:\; 302.5 \leq v^{o} \leq 744.0 \;.$$

It can now be reasoned that assignment of initial data, uniform over the entire solution domain (4.24), from [R1] will cause convergence

of the iterative scheme to the subsonic root of (4.27), or (4.28) at each duct location. This will then give the subsonic axial fluid speed variation for that particular motion. Similarly assignment of uniform initial data within [R2] will give the supersonic axial fluid speed variation.

The iteration of the axial fluid speed variation of both flow types for both motions is now started from the constant initial data,

$$\begin{aligned} &\text{SUBSONIC FLOW} \quad : \quad v^{o} = 200.0 \qquad 0.0 \leq x \leq 1.0 \ , \\ &\text{SUPERSONIC FLOW} \quad : \quad v^{o} = 500.0 \qquad 0.0 \leq x \leq 1.0 \ , \end{aligned} \tag{4.33}$$

in accordance with (4.32). The qualitative behaviour of the fluid speeds, i.e. the roots, is available from the corresponding graphs (FIG.4). It can be seen that all such values for both motions lie within the open interval $(87,\alpha)$, and thus if the initial data can be additionally specified such that it is sufficiently close to the respective root then this will ensure quadratic convergence of the iterative method.

The axial fluid speed variation for flow through the converging section, subsonically and supersonically, is shown in FIGS.10ii,ix and for the diverging section in FIG.11ii,ix. These respective parameterizations may then be used to determine the axial variation of the remaining flow variables, for each flow type in each motion, through the algebraic relations (1.18) and (1.23)-(1.26) (see FIGS.10,11).

Furthermore, each of the respective fluid speed variations may subsequently be taken as an intermediate numerical parameterization in these algebraic relations to provide the remaining inter-variable variations applicable to the particular motion, in the same manner as was performed for a general stream-line in (§1).

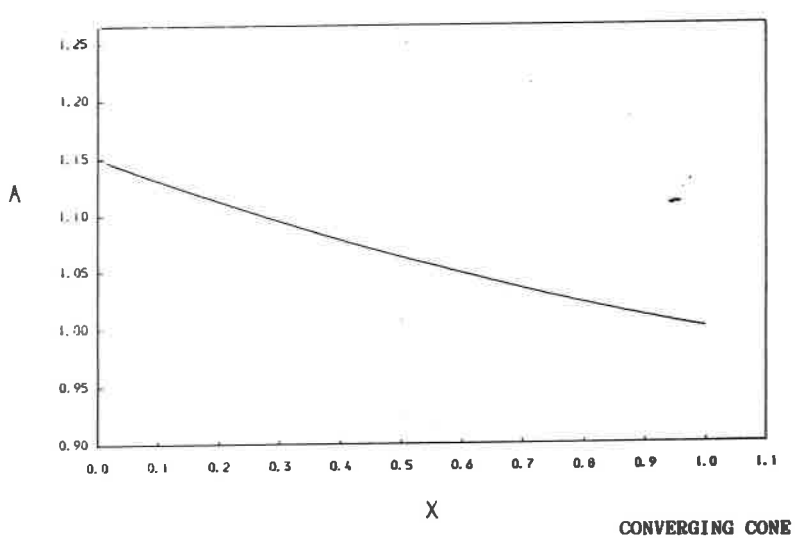

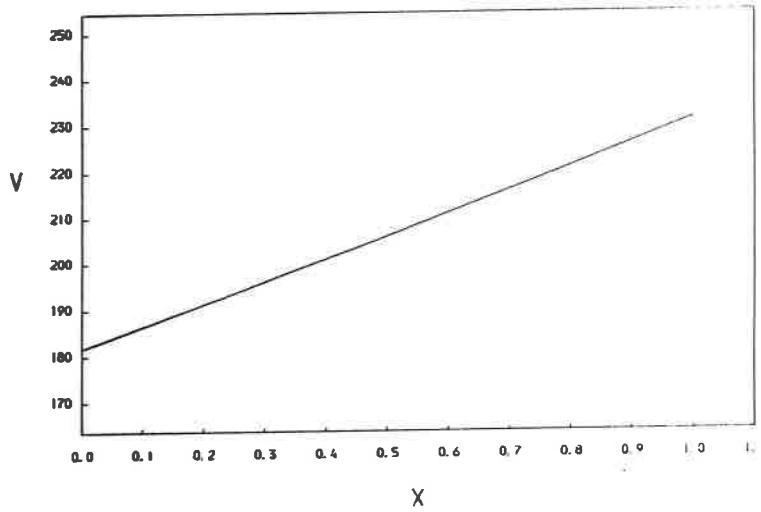

CONVERGING CONE SECTION : SUBSONIC FLOW

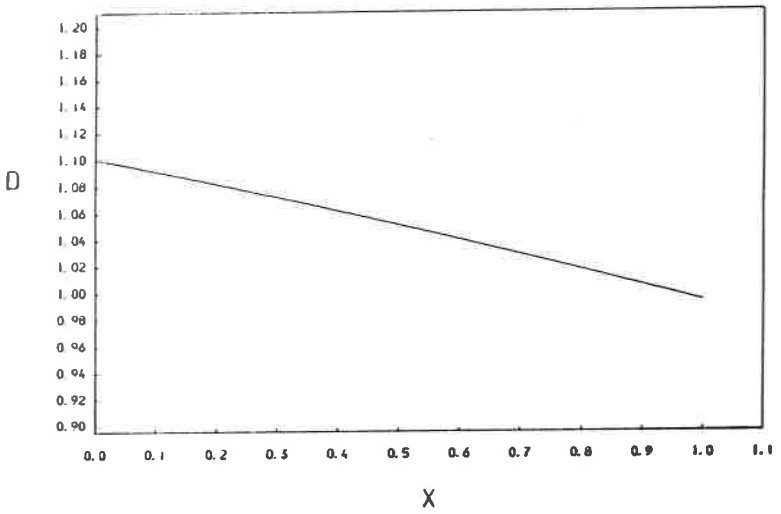

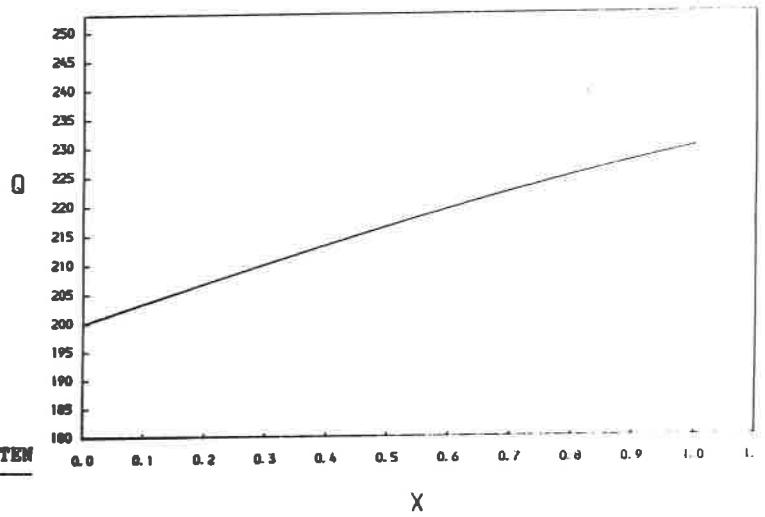

FIG TEN

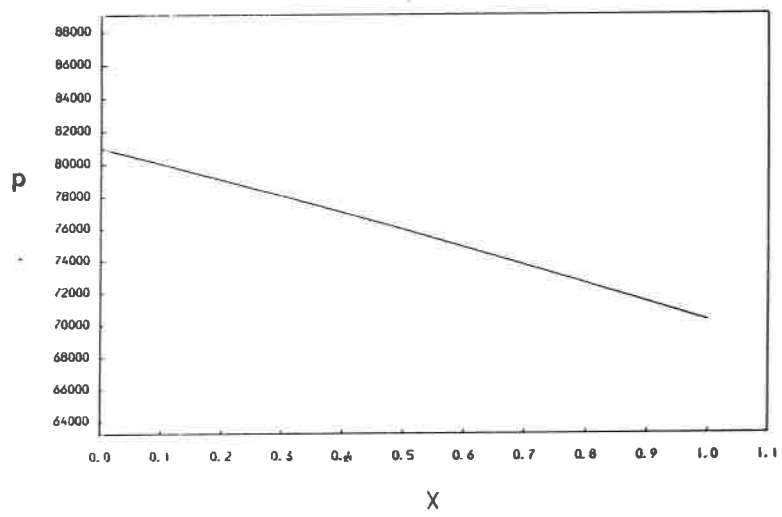
p
88000
86000
84000
82000
80000
78000
76000
74000
72000
70000
68000
66000
64000
0.0 0.1 0.2 0.3 0.4 0.5 0.6 0.7 0.8 0.9 1.0 1.1
X

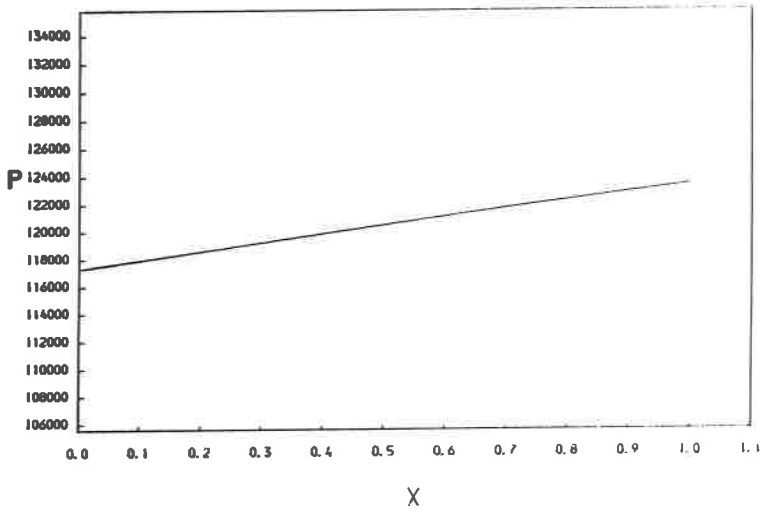
P
134000
132000
130000
128000
126000
124000
122000
120000
118000
116000
114000
112000
110000
108000
106000
0.0 0.1 0.2 0.3 0.4 0.5 0.6 0.7 0.8 0.9 1.0 1.1
X

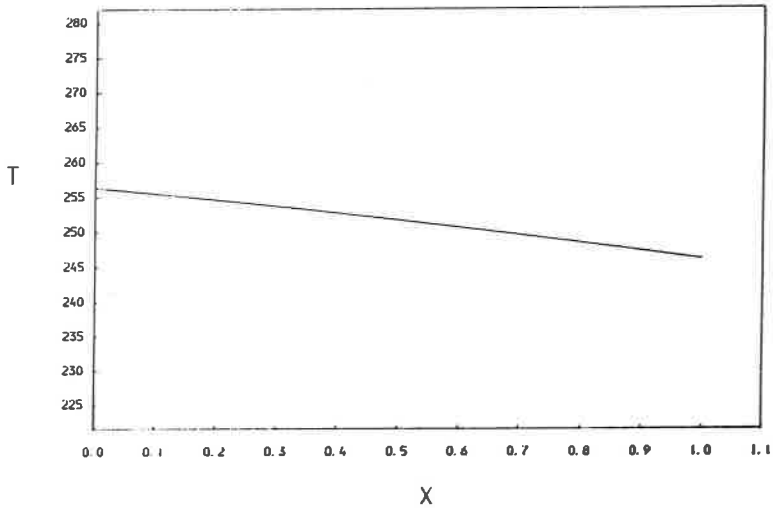
T
280
275
270
265
260
255
250
245
240
235
230
225
0.0 0.1 0.2 0.3 0.4 0.5 0.6 0.7 0.8 0.9 1.0 1.1
X

FIG TEN

cont.

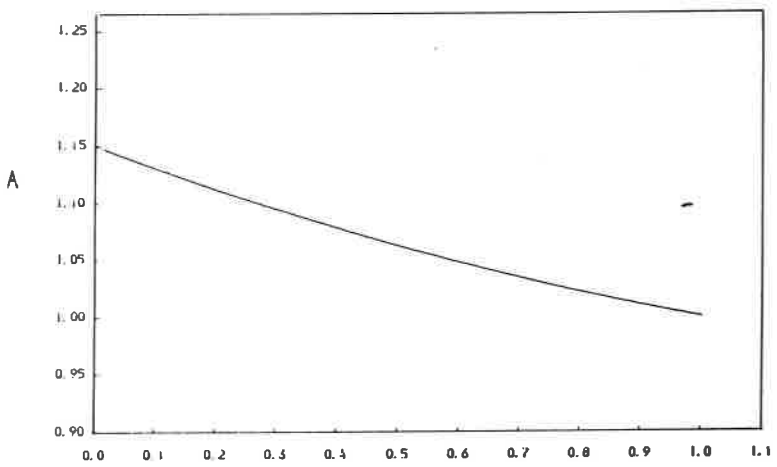

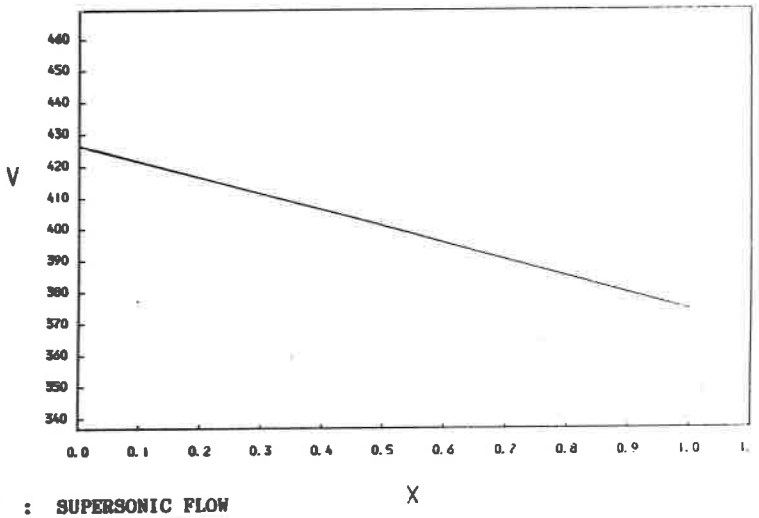

CONVERGING CONE SECTION : SUPERSONIC FLOW

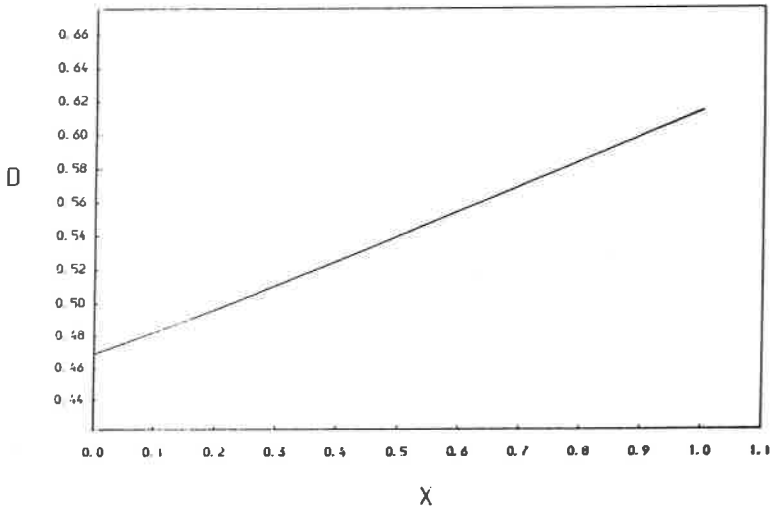

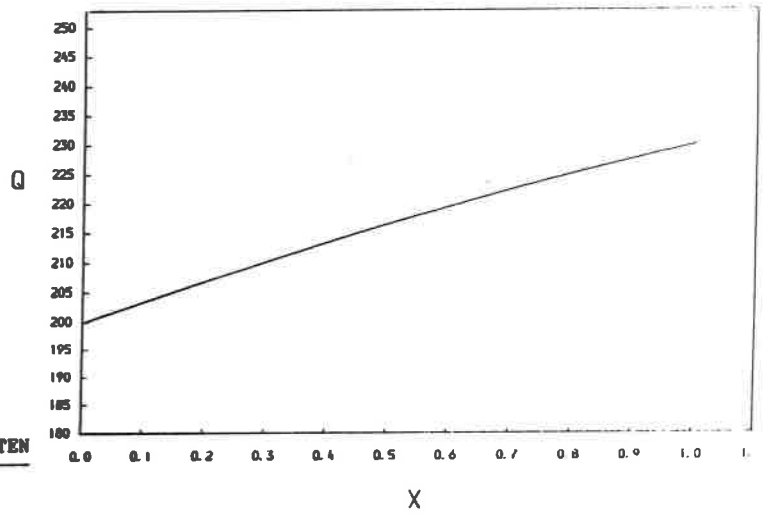

FIG TEN

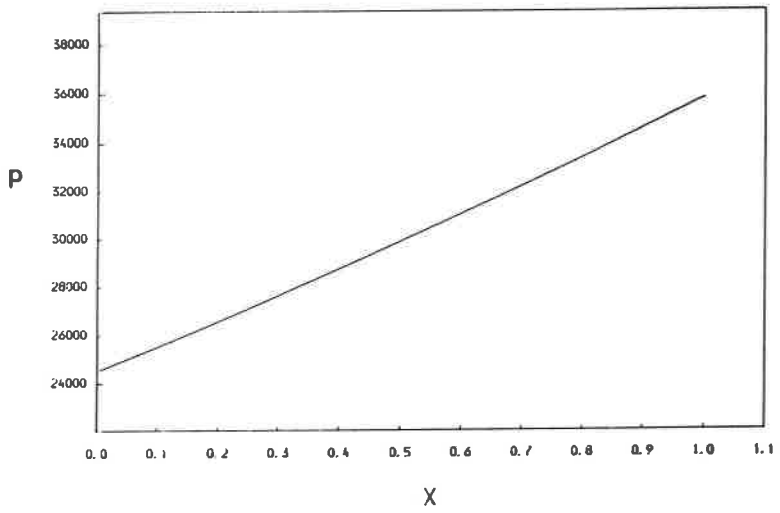
P
38000
36000
34000
32000
30000
28000
26000
24000
0.0 0.1 0.2 0.3 0.4 0.5 0.6 0.7 0.8 0.9 1.0 1.1
X

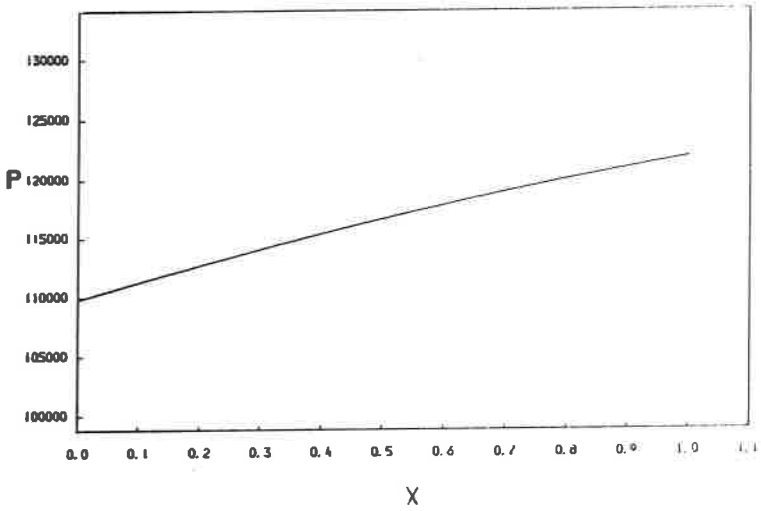
P
130000
125000
120000
115000
110000
105000
100000
0.0 0.1 0.2 0.3 0.4 0.5 0.6 0.7 0.8 0.9 1.0 1.1
X

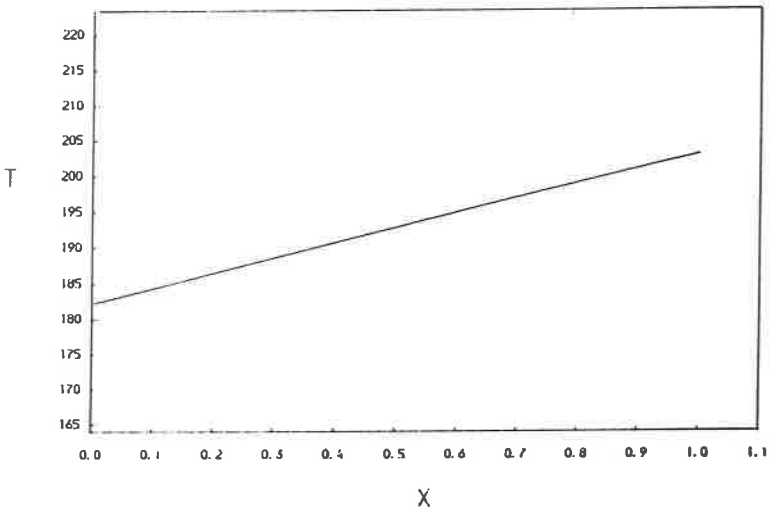
T
220
215
210
205
200
195
190
185
180
175
170
165
0.0 0.1 0.2 0.3 0.4 0.5 0.6 0.7 0.8 0.9 1.0 1.1
X

FIG TEN

cont.

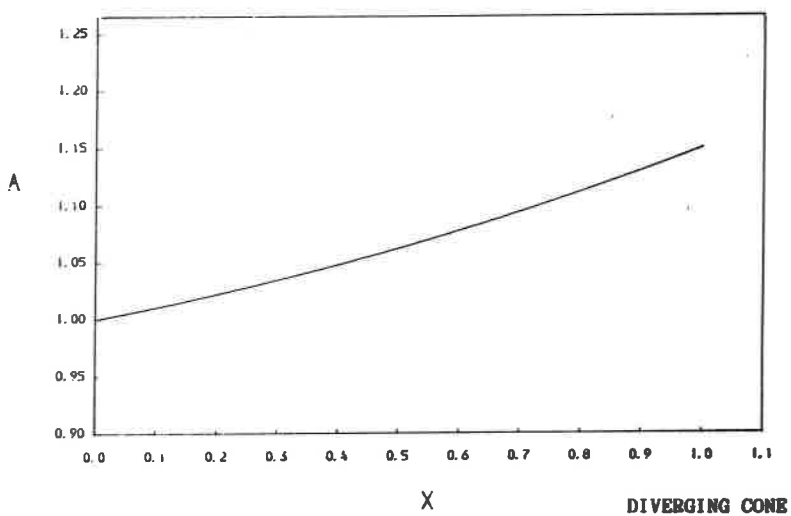

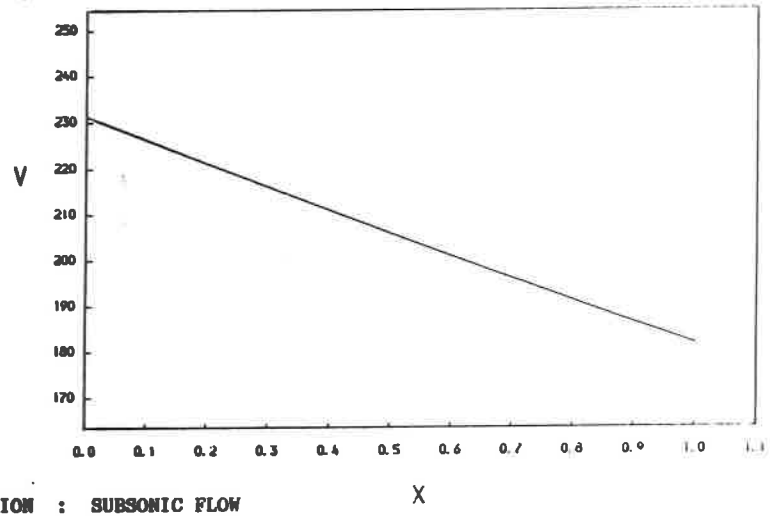

DIVERGING CONE SECTION : SUBSONIC FLOW

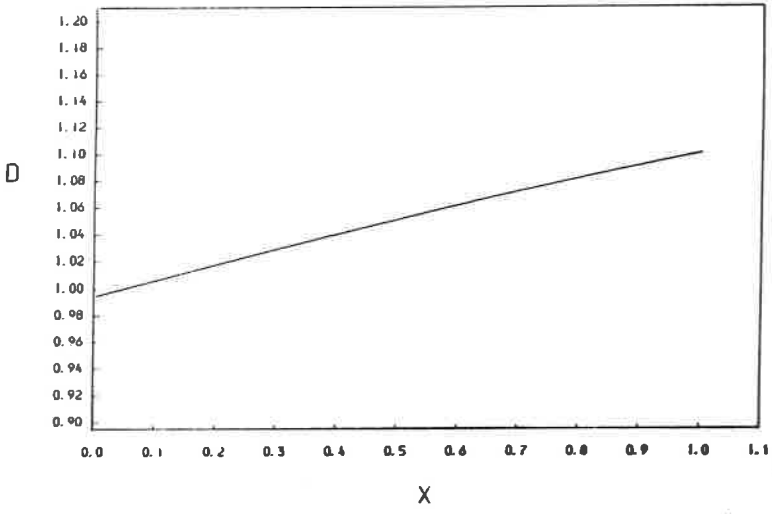

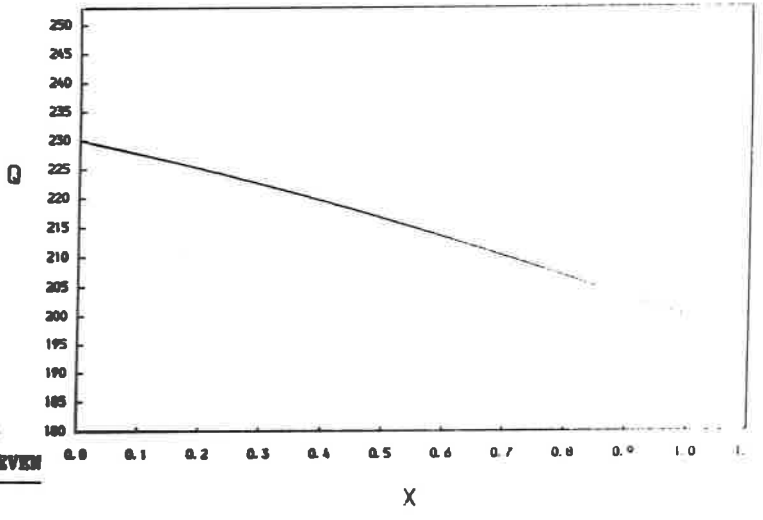

FIG ELEVEN

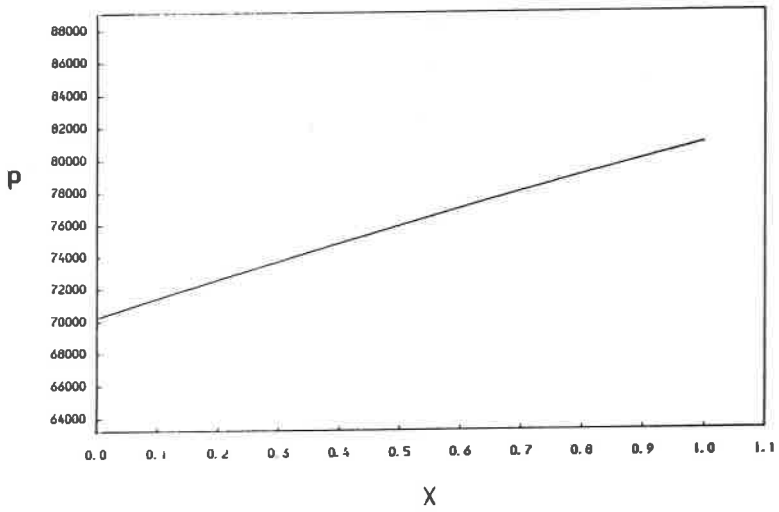

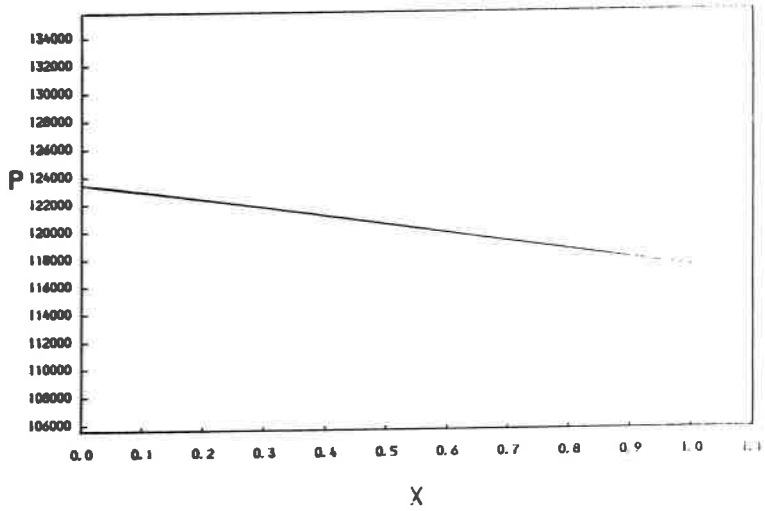

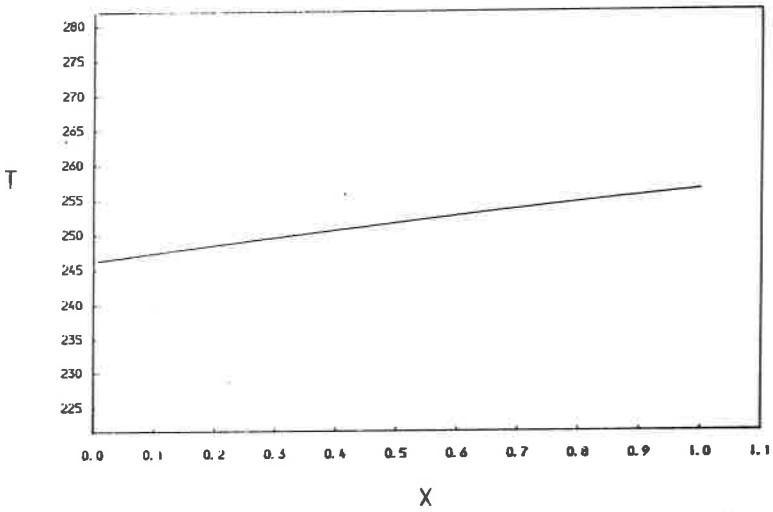

FIG ELEVEN

cont.

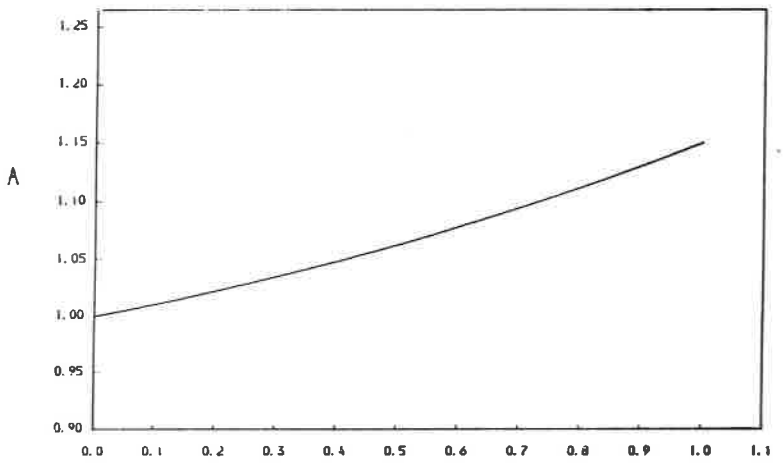

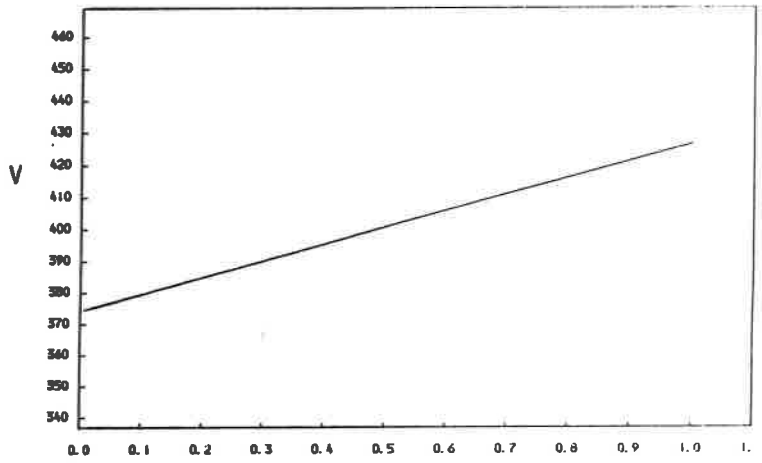

DIVERGING CONE SECTION : SUPERSONIC FLOW

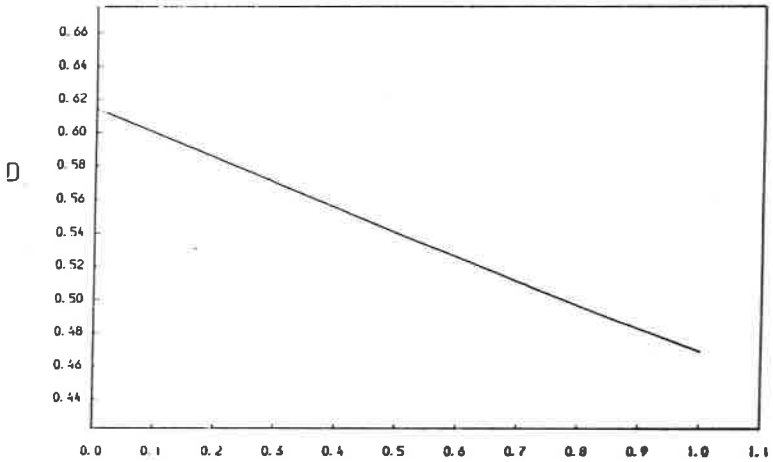

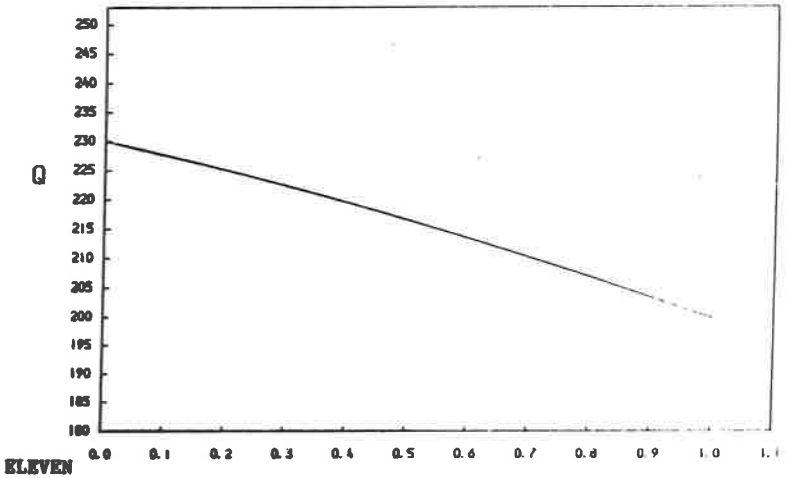

FIG ELEVEN

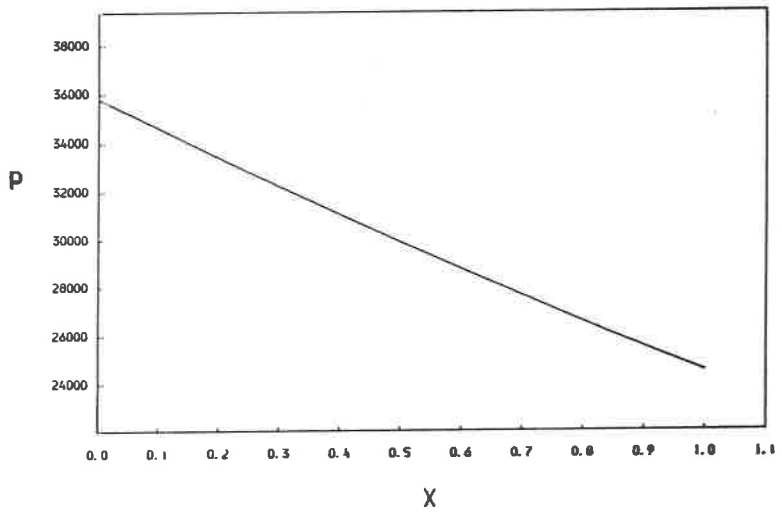

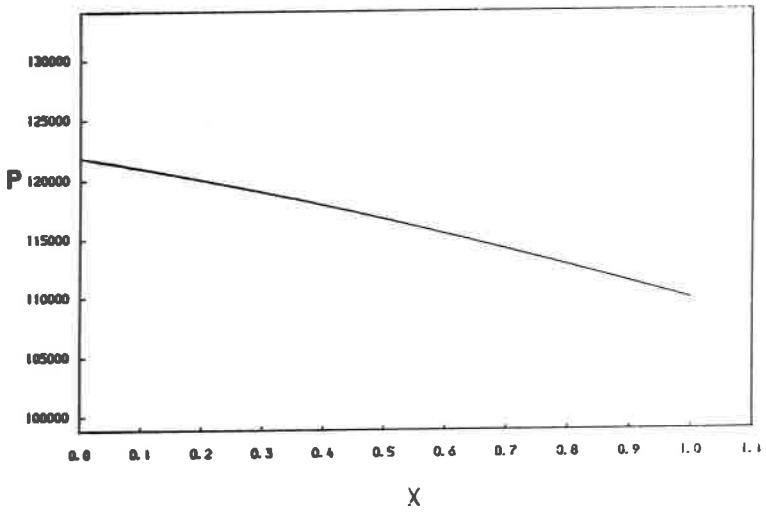

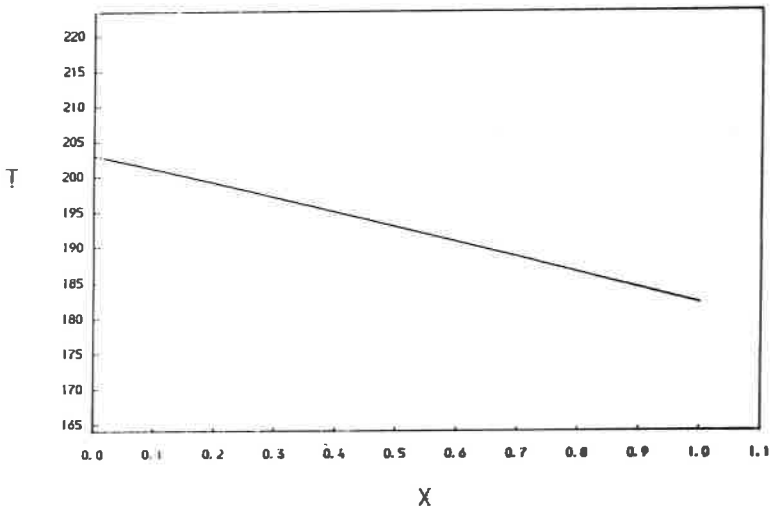

FIG ELEVEN

cont.

4.4 NOZZLE FLOW PARAMETERIZATION

For determination of the nozzle axial fluid speed variation for a particular motion, let the domain of solution, on which the nozzle lies, be,

$$0.0 \leq x \leq 2.0 \ . \tag{4.34}$$

The particular motion to be considered is defined by (3.27), (3.28) and the area variation by

$$\begin{aligned} A_1(x) &= 1.1 - (x/8.0) \qquad 0.0 \leq x \leq 0.8 \ , \\ A_2(x) &= (2.6/3.0) + (x/6.0) \qquad 0.8 \leq x \leq 2.0 \ , \end{aligned} \tag{4.35}$$

(see FIG.12i).

The particular non-linear relation between fluid speed and axial nozzle location is then in two parts associated with the nozzle entry section and exhaust section (diffuser),

$$F_1(v) = v^2 - 2\,h\,v^{0.4} + 7\,\eta \left[\frac{246.31124}{1.1 - (x/8.0)} \right] , \tag{4.36}$$

$$F_2(v) = v^2 - 2\,h\,v^{0.4} + 7\,\eta \left[\frac{246.31124}{(2.6/3.0) + (x/6.0)} \right] , \tag{4.37}$$

respectively, again with the flow constants taking the values (1.30) and (1.31).

The convergence condition (4.18) [with (4.19) in its associated form] must bound the initial data at each of the 201 uniformly spaced nozzle locations if Newton's method is to converge. TABLE.3 here gives a sample of these axial positions and associated bounding intervals, the intersection of which, namely

$$\text{DE-LAVAL NOZZLE FLOW} \;:\; [10,776]\,, \qquad (4.38)$$

provides a guideline for the assignment of the uniform initial data values over the complete solution domain.

DE-LAVAL NOZZLE	BOUNDING INITIAL DATA INTERVALS	
DOMAIN LOCATION x	NOZZLE AREA A(x)	BOUNDING INTERVAL $[\alpha,\beta]$
0.0	1.1	[10,786]
0.8	1.0	[10,798]
2.0	1.2	[9,776]

TABLE THREE

In the same manner as for section flow it is found that the

intersection interval (4.38) may again be split into two distinct internal initial data regions, again divided by the critical fluid speed (1.33),

$$\text{[R1]} \quad 10.0 \leq v^{o} < 302.5 \ ,$$

and (4.39)

$$\text{[R2]} \quad 302.5 \leq v^{o} \leq 776.0 \ .$$

The assignment of initial data is taken to be

$$\begin{aligned} &\text{SUBSONIC FLOW} \quad : \quad v^{o} = 200.0 \qquad 0.0 \leq x \leq 2.0 \ , \\ &\text{TRANSITION FLOW} \quad : \quad v^{o} = 200.0 \qquad 0.0 \leq x \leq 0.8 \\ &\qquad\qquad\qquad\quad\ \ v^{o} = 500.0 \qquad 0.8 < x \leq 2.0 \ , \end{aligned} \tag{4.40}$$

uniform over the solution domain (4.34). From [R1] this will be expected to provide convergence at each axial location, of the iterative method to the subsonic root of the appropriate function (dependent on in which section of the nozzle this position lies) and correspondingly if from [R2] to the supersonic root.

The qualitative behaviour of the roots is again available from the graphs (FIGS.8,9). These roots lie within the open interval $(87,\alpha)$ and thus the particular initial data specified takes into account not only the required flow type through the nozzle, but also allows the possibility of quadratic convergence of the iterative scheme.

The subsonic axial fluid speed variation is shown in FIG.12 and the transition axial fluid speed variation in FIG.13. Once again these parameterizations may subsequently be used in the determination of the axial variation of the other flow variables for both flow behaviours through the algebraic relations (1.18) and (1.23)-(1.26) (see FIGS.12,13).

The remaining approximate inter-variable relations for each flow behaviour, analagous to (§1), may then be obtained by the use of each fluid speed variation as an intermediate numerical parameterization in the same algebraic relations.

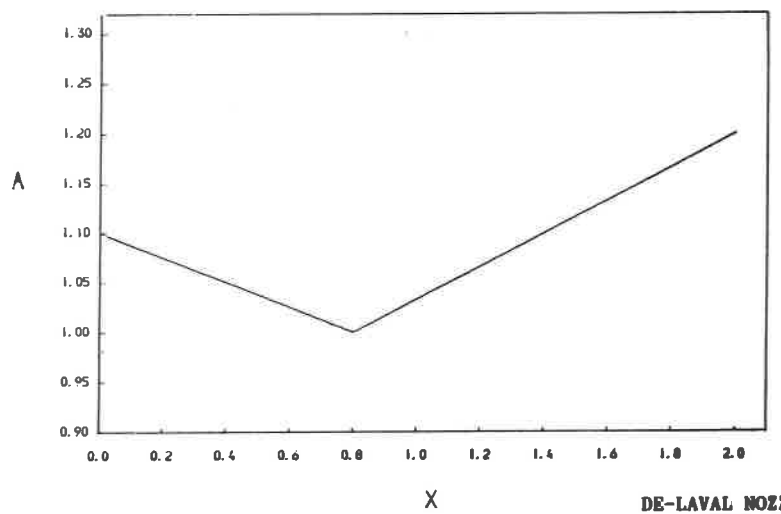

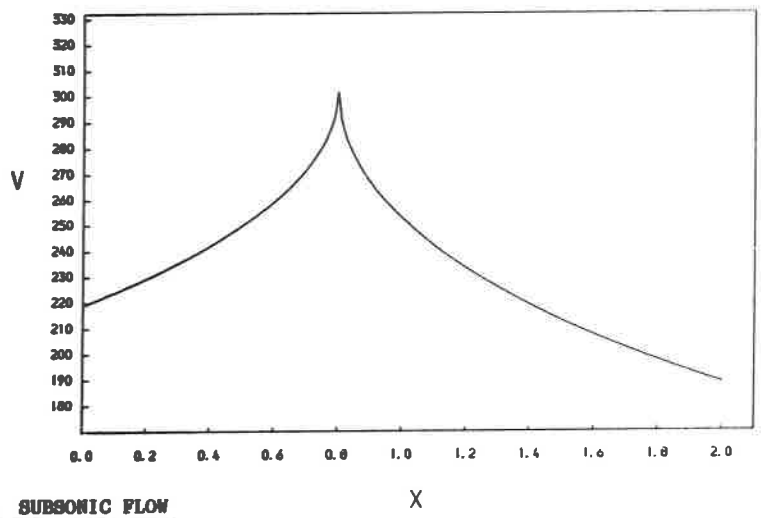

DE-LAVAL NOZZLE : SUBSONIC FLOW

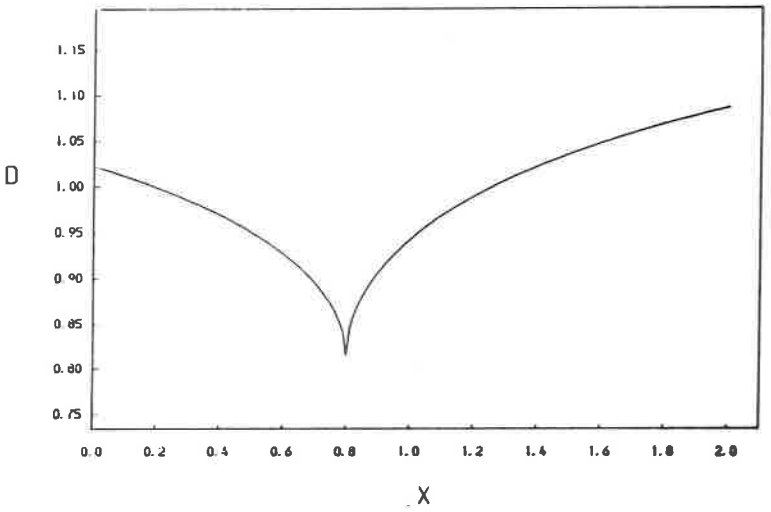

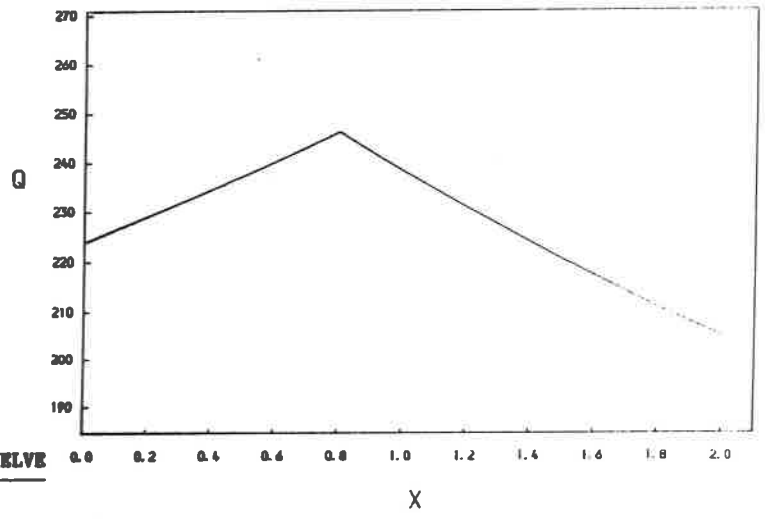

FIG TWELVE

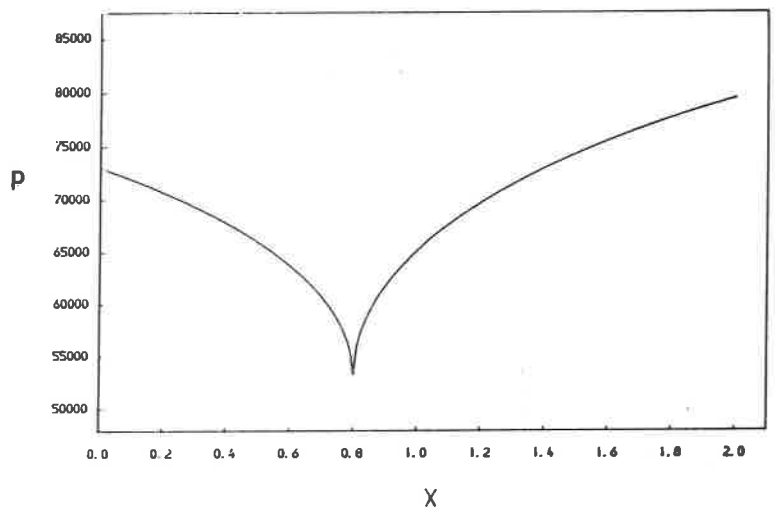

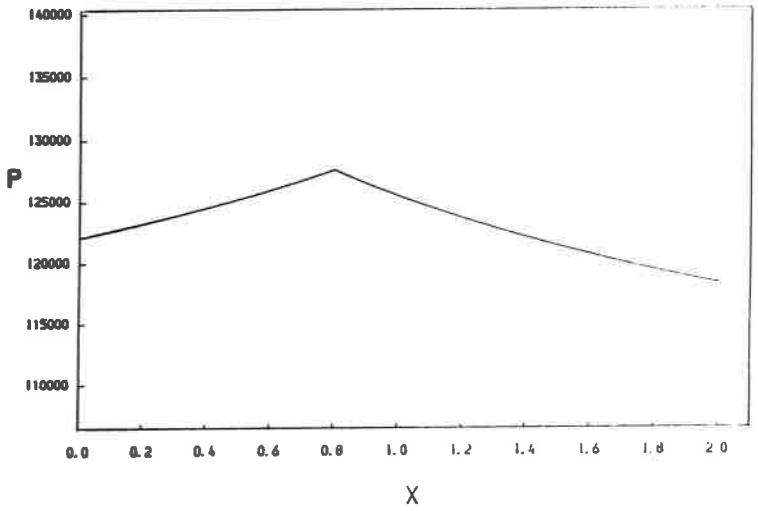

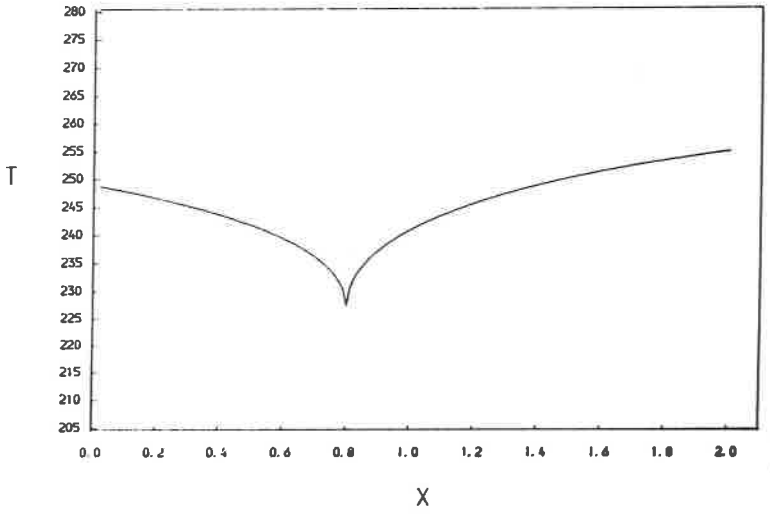

FIG TWELVE

cont.

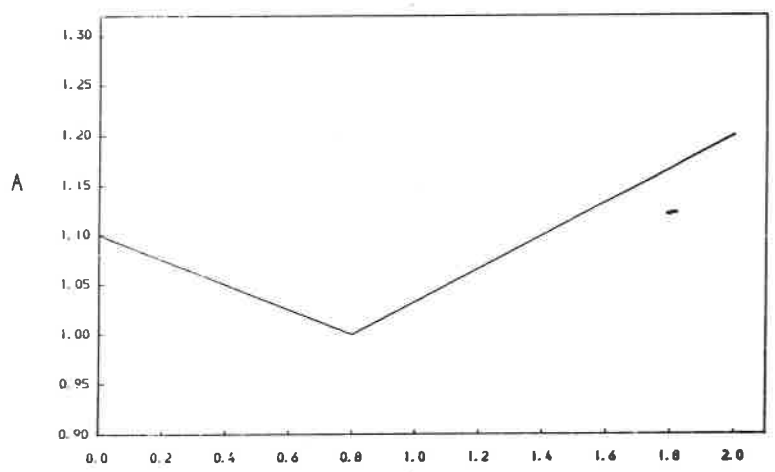

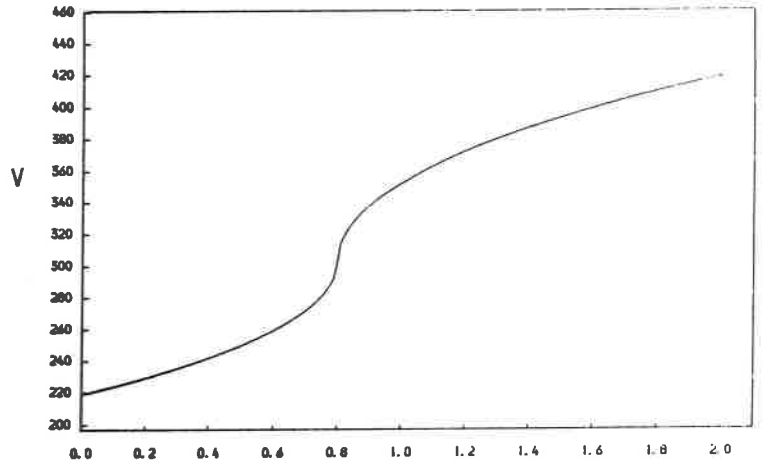

DE-LAVAL NOZZLE : TRANSITION FLOW

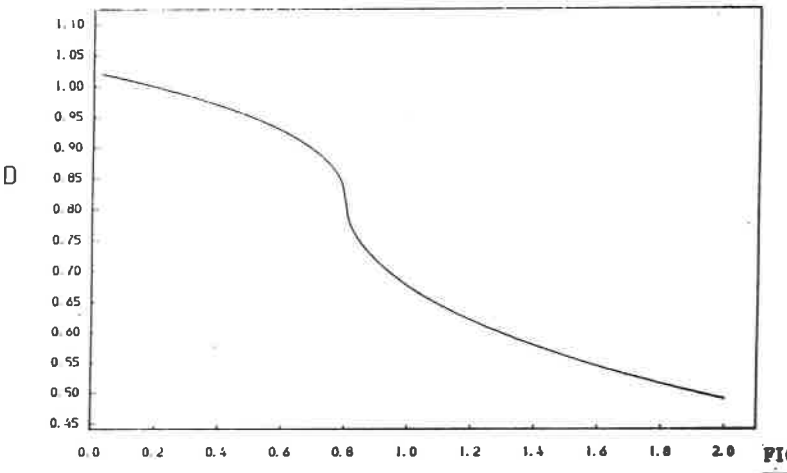

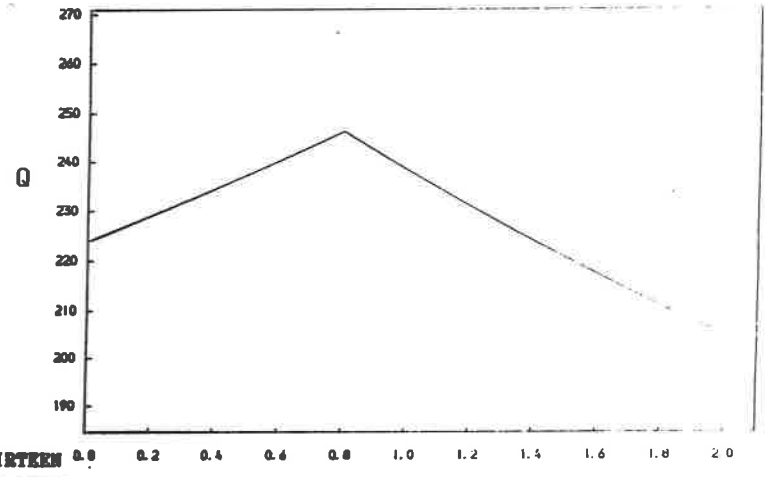

FIG THIRTEEN

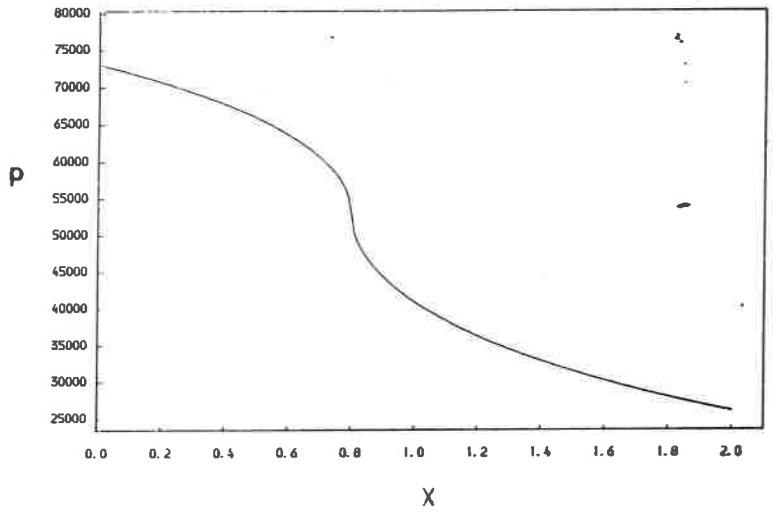

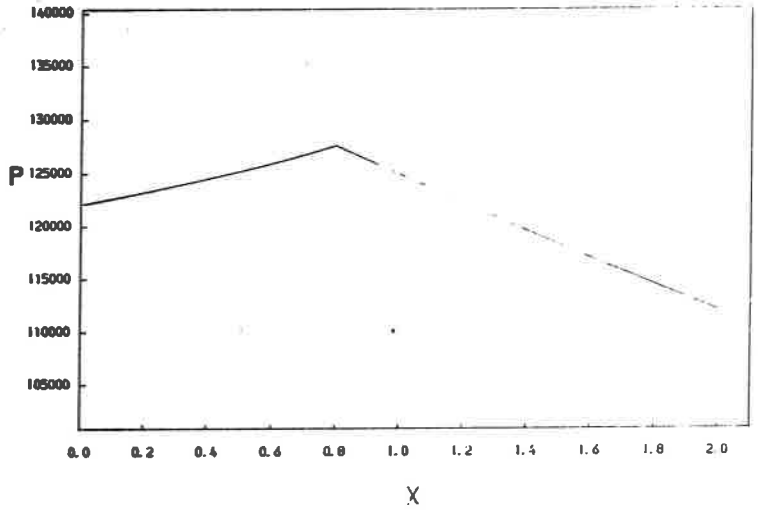

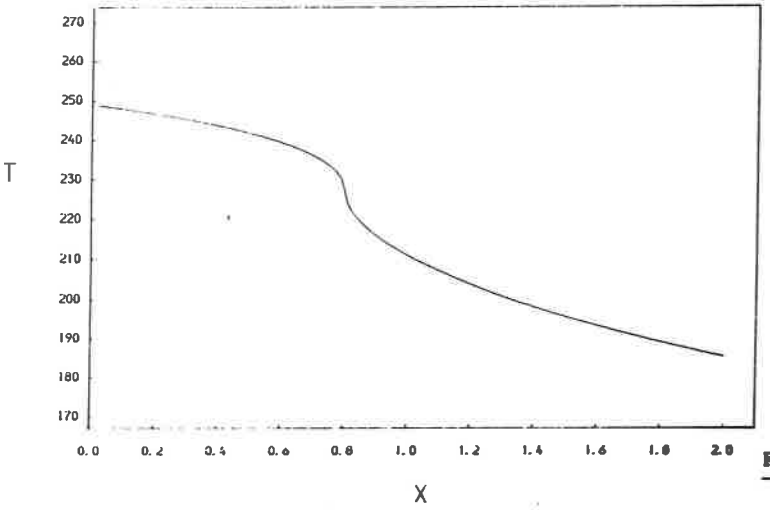

FIG THIRTEEN

cont.

4.5 SUMMARY

An algebraic formulation for the determination of the axial flow variable variation in quasi one-dimensional primary duct flow has been examined.

A key factor is that Bernouilli's equation in the form (4.2) holds on a streamline which is representative of the full duct flow. When combined with the map (2.6), relating position along the duct axis to local mass flow rate, a parameterization of the flow variables, in terms of position, is provided, which gives insight into their behaviour.

The non-linear relation connecting velocity and axial distance is solved at a discrete number of points throughout the duct by the Newton iterative algorithm, paying special attention to the convergence conditions. The axial variation of the remaining flow variables can then be simply computed.

REFERENCES

[1] COURANT, R. & FRIEDRICHS, K.O. : "Supersonic Flow And Shock Waves", INTER-SCIENCE, NEW YORK (1948).

[2] SEWELL, M.J. : "Properties Of A Streamline In Gas Flow", PHYS. TECHNOL. 16, (1985).

[3] PORTER, D. & SEWELL, M.J. : Constitutive Surfaces In Fluid Dynamics", DEPT. OF MATHS., UNIV. OF READING (1979).

[4] SPIVAK, M. : "Calculus", W.A. BENJAMIN INC., LONDON (1967).

[5] JOHNSON, L.W. & RIESS, R.D. : "Numerical Analysis", 2nd Ed., ADDISON-WESLEY (1982).